

**International
Journal of
Engineering
Technologies
(IJET)**

Printed ISSN: 2149-0104

e-ISSN: 2149-5262

Volume: 1

No: 3

September 2015

© Istanbul Gelisim University Press, 2015

Certificate Number: 23696

All rights reserved.

International Journal of Engineering Technologies is an international peer-reviewed journal and published quarterly. The opinions, thoughts, postulations or proposals within the articles are but reflections of the authors and do not, in any way, represent those of the Istanbul Gelisim University.

CORRESPONDENCE and COMMUNICATION:

Istanbul Gelisim University Faculty of Engineering and Architecture
Cihangir Mah. Şehit P. Onb. Murat Şengöz Sk. No: 8
34315 Avcilar / Istanbul / TURKEY
Phone: +90 212 4227020 Ext. 221
Fax: +90 212 4227401
e-Mail: ijet@gelisim.edu.tr
Web site: <http://ijet.gelisim.edu.tr>
<http://dergipark.ulakbim.gov.tr/ijet>


Printing and binding:

Anka Matbaa
Sertifika No: 12328
Tel: +90 212 5659033 - 4800571
e-Posta: ankamatbaa@gmail.com

International Journal of Engineering Technologies (IJET) is included in:



**International Journal of Engineering Technologies (IJET) is indexed
by the following service:**

Organization	URL	Starting Date	Feature
 OpenAIRE The OpenAIRE2020 Project	https://www.openaire.eu/	2015	Open Access



INTERNATIONAL JOURNAL OF ENGINEERING TECHNOLOGIES (IJET)
International Peer-Reviewed Journal
Volume 1, No 3, September 2015, Printed ISSN: 2149-0104, e-ISSN: 2149-5262

Owner on Behalf of Istanbul Gelisim University
Rector Prof. Dr. Burhan AYKAÇ

Editor-in-Chief
Prof. Dr. İlhami ÇOLAK

Associate Editors
Dr. Selin ÖZÇİRA
Dr. Mehmet YEŞİLBUDAK

Layout Editor
Seda ERBAYRAK

Proofreader
Özlemnur ATAOL

Copyeditor
Evrin GÜLEY

Contributor
Ahmet Şenol ARMAĞAN

Cover Design
Tarık Kaan YAĞAN

Editorial Board

Professor İlhami COLAK, Istanbul Gelisim University, Turkey

Professor Dan IONEL, Regal Beloit Corp. and University of Wisconsin Milwaukee, United States

Professor Fujio KUROKAWA, Nagasaki University, Japan

Professor Marija MIROSEVIC, University of Dubrovnik, Croatia

Prof. Dr. Şeref SAĞIROĞLU, Gazi University, Graduate School of Natural and Applied Sciences, Turkey

Professor Adel NASIRI, University of Wisconsin-Milwaukee, United States

Professor Mamadou Lamina DOUMBIA, University of Québec at Trois-Rivières, Canada

Professor João MARTINS, University/Institution: FCT/UNL, Portugal

Professor Yoshito TANAKA, Nagasaki Institute of Applied Science, Japan

Dr. Youcef SOUFI, University of Tébessa, Algeria

Prof.Dr. Ramazan BAYINDIR, Gazi Üniversitesi, Turkey

Professor Goce ARSOV, SS Cyril and Methodius University, Macedonia

Professor Tamara NESTOROVIĆ, Ruhr-Universität Bochum, Germany

Professor Ahmed MASMOUDI, University of Sfax, Tunisia

Professor Tsuyoshi HIGUCHI, Nagasaki University, Japan

Professor Abdelghani AISSAOUI, University of Bechar, Algeria

Professor Miguel A. SANZ-BOBI, Comillas Pontifical University /Engineering School, Spain

Professor Mato MISKOVIĆ, HEP Group, Croatia

Professor Nilesh PATEL, Oakland University, United States

Assoc. Professor Juan Ignacio ARRIBAS, Universidad Valladolid, Spain

Professor Vladimir KATIC, University of Novi Sad, Serbia

Professor Takaharu TAKESHITA, Nagoya Institute of Technology, Japan

Professor Filote CONSTANTIN, Stefan cel Mare University, Romania

Assistant Professor Hulya OBDAN, Istanbul Yildiz Technical University, Turkey

Professor Luis M. San JOSE-REVUELTA, Universidad de Valladolid, Spain

Professor Tadashi SUETSUGU, Fukuoka University, Japan

Associate Professor Zehra YUMURTACI, Istanbul Yildiz Technical University, Turkey

Dr. Rafael CASTELLANOS-BUSTAMANTE, Instituto de Investigaciones Eléctricas, Mexico

Assoc. Prof. Dr. K. Nur BEKIROGLU, Yildiz Technical University, Turkey

Professor Gheorghe-Daniel ANDREESCU, Politehnica University of Timisoara, Romania

Dr. Jorge Guillermo CALDERÓN-GUIZAR, Instituto de Investigaciones Eléctricas, Mexico

Professor VICTOR FERNÃO PIRES, ESTSetúbal/Polytechnic Institute of Setúbal, Portugal

Dr. Hiroyuki OSUGA, Mitsubishi Electric Corporation, Japan

Associate Professor Serkan TAPKIN, Istanbul Gelisim University, Turkey

Professor Luis COELHO, ESTSetúbal/Polytechnic Institute of Setúbal, Portugal

Professor Furkan DINCER, Mustafa Kemal University, Turkey

Professor Maria CARMEZIM, ESTSetúbal/Polytechnic Institute of Setúbal, Portugal

Associate Professor Lale T. ERGENE, Istanbul Technical University, Turkey

Dr. Hector ZELAYA, ABB Corporate Research, Sweden

Professor Isamu MORIGUCHI, Nagasaki University, Japan

Associate Professor Kiruba SIVASUBRAMANIAM HARAN, University of Illinois, United States

Associate Professor Leila PARSA, Rensselaer Polytechnic Institute, United States

Professor Salman KURTULAN, Istanbul Technical University, Turkey

Professor Dragan ŠEŠLIJA, University of Novi Sad, Serbia

Professor Birsen YAZICI, Rensselaer Polytechnic Institute, United States

Assistant Professor Hidenori MARUTA, Nagasaki University, Japan

Associate Professor Yilmaz SOZER, University of Akron, United States

Associate Professor Yuichiro SHIBATA, Nagasaki University, Japan

Professor Stanimir VALTCHEV, Universidade NOVA de Lisboa, (Portugal) + Burgas Free University, (Bulgaria)

Professor Branko SKORIC, University of Novi Sad, Serbia

Dr. Cristea MIRON, Politehnica University in Bucharest, Romania

Dr. Nobumasa MATSUI, MHPS Control Systems Co., Ltd, Japan

Professor Mohammad ZAMI, King Fahd University of Petroleum and Minerals, Saudi Arabia

Associate Professor Mohammad TAHA, Rafik Hariri University (RHU), Lebanon

Assistant Professor Kyungnam KO, Jeju National University, Republic of Korea

Dr. Guray GUVEN, Conductive Technologies Inc., United States

Dr. Tuncay KAMAŞ, Eskişehir Osmangazi University, Turkey

From the Editor

Dear Colleagues,

On behalf of the editorial board of International Journal of Engineering Technologies (IJET), I would like to share our happiness to publish the third issue of IJET. My special thanks are for members of editorial board, editorial team, referees, authors and other technical staff.

Please find the third issue of International Journal of Engineering Technologies at <http://dergipark.ulakbim.gov.tr/ijet>. We invite you to review the Table of Contents by visiting our web site and review articles and items of interest. IJET will continue to publish high level scientific research papers in the field of Engineering Technologies as an international peer-reviewed scientific and academic journal of Istanbul Gelisim University.

Thanks for your continuing interest in our work,

Professor ILHAMI COLAK
Istanbul Gelisim University
icolak@gelisim.edu.tr

<http://dergipark.ulakbim.gov.tr/ijet>
Printed ISSN: 2149-0104
e-ISSN: 2149-5262

International Journal of
Engineering Technologies
IJET

Table of Contents

	Page
<i>From the Editor</i>	<i>vii</i>
<i>Table of Contents</i>	<i>ix</i>
<hr/>	
<u>Different Implementation Approaches of the Strong Form Meshless Implementation of Taylor Series Method</u>	
<i>Armagan Karamanli</i>	95-105
<u>Flow Visualization of Sloshing in an Accelerated 2-D Rectangular Tank</u>	
<i>Gurhan Sahin, Seyfettin Bayraktar</i>	106-112
<u>A Comparison of Experimental and Estimated Data Analyses of Solar Radiation, in Adiyaman, Turkey</u>	
<i>Haci Sogukpinar, Ismail Bozkurt, Nazif Calis</i>	113-117
<u>Modelling of Instant Solar Radiation Using Average Instant Temperature of Ogbomoso, South Western, Nigeria</u>	
<i>Oluwaseun Adedokun, Aishat Abidemi Abass, Yekinni Kolawole Sanusi</i>	118-122

International Journal of Engineering Technologies, IJET

e-Mail: ijet@gelisim.edu.tr
Web site: <http://ijet.gelisim.edu.tr>
<http://dergipark.ulakbim.gov.tr/ijet>

Different Implementation Approaches of the Strong Form Meshless Implementation of Taylor Series Method

Armagan Karamanli*[‡]

*Research and Development Department, TIRSAN Treyler Sanayi ve Ticaret A.S., Sancaktepe, Istanbul, Turkey
(armagan_k@yahoo.com)

[‡]Corresponding Author; Armagan Karamanli, Osmangazi Mah., Yıldızhan Cad., No:4, 3488, Sancaktepe, Istanbul, Turkey
Tel:+90 216 564 0200, Fax: +90 216 311 7156, armagan_k@yahoo.com

Received: 22.06.2015 Accepted: 08.08.2015

Abstract-Based on the Taylor series expansion (TSE) and employing the technique of differential transform method (DTM), three new meshless approaches which are called Meshless Implementation of Taylor Series Methods (MITSM) are presented. In particular, Strong Form Meshless Implementation of Taylor Series Methods (SMITSM) are studied in this paper. Then, the basic functions are used to solve a 1D second-order ordinary differential equation and 2D Laplace equation by using the SMITSM. Comparisons are made with the analytical solutions and results of Symmetric Smoothed Particle Hydrodynamics (SSPH) method. We also compared the effectiveness of the SMITSM and SSPH method by considering various particle distributions, nonhomogeneous terms and number of terms in the basic functions. It is observed that the MITSM has the conventional convergence properties and, at the expense of CPU time, yields smaller L_2 error norms than the SSPH method, especially in the existence of nonsmooth nonhomogeneous problems.

Keywords: Meshless methods, Taylor series, element free method, strong form, heat transfer, differential transform method.

1. Introduction

Meshless Smoothed Particle Hydrodynamics (SPH) method, proposed by Lucy [1] to study three-dimensional (3D) astrophysics problems, has been successfully applied to analyze transient fluid and solid mechanics problems. However, it has two shortcomings such as inaccuracy at particles on the boundary and tensile instability. Many techniques have been developed to alleviate these two deficiencies among which are Corrected Smoothed Particle Method (CSPM) [2, 3], Reproducing Kernel Particle Method (RKPM) [4-6] and Modified Smoothed Particle Hydrodynamics (MSPH) method [7-10]. The MSPH method has been successfully applied to study wave propagation in functionally graded materials [9], can capture the stress field near a crack-tip, and simulates the propagation of multiple cracks in a linear elastic body [10]. The SSPH method has been applied to 2D homogeneous elastic problem successfully [11]. On the other hand, the SSPH method [11-13] is more suitable for homogeneous boundary value problems, cannot be easily applicable to nonlinear problems, requires at least fourth order terms in basis functions for the buckling problems which increases the CPU time.

Motivated by the fact that the SSPH method may not yield accurate results for solving nonhomogeneous problems due to its underlying formulation, an alternative approach is investigated especially for nonhomogeneous problems [14]. Three different implementations of MITSM including the approach presented in [14], called Meshless Implementation of Taylor Series Method I, II and III (MITSM) are presented in this paper.

The method presented in [14] requires all derivatives of the kernel function which restricts the choice of the kernel function and only uses all derivatives of the basis function. However, Meshless Implementation of Taylor Series Method I does not require the derivatives of the kernel function and may use any type of kernel function including a constant. On the other hand, Taylor Series Method II uses all derivatives of both basis and kernel functions.

Although the SSPH method and MITSM depend on TSEs, the main difference between these two approaches is as follows: the SSPH method calculates the value of the solution at a node by using the values of the solution at the other nodes and then substitute it into the governing differential equation; thus, nonhomogeneous terms in the

governing differential equation are also evaluated pointwise at the nodes. This approach results in approximation errors especially in the existence of nonsmooth nonhomogeneous terms. On the other hand, the proposed MITSM approach substitute the TSEs of the solution and nonhomogeneous term into the governing differential equation and then utilize exact recursive relations between the coefficients of the expansions of the solution and nonhomogeneous term; it yields improvement in accuracy that is verified by solving numerical examples in Section 4. The MITSM can be applied to arbitrary boundary geometries, nonlinear problems, and strong and weak formulations. In particular, Strong Form Meshless Implementation of Taylor Series Methods (SMITSM) are investigated in this paper, whose results are compared with the analytical solutions and solutions of the SSPH method. It is shown that the two of SMITSM has the conventional convergence properties and yields smaller L_2 error norms in numerical examples than the SSPH method, especially in the existence of nonsmooth nonhomogeneous terms.

2. Differential Transform Method

In this study, the DTM technique is employed to develop the MITSM. It is noteworthy that when the DTM is applied to ordinary differential equations, it exactly coincides with the traditional Taylor series method [15] where applications of TSEs and DTM are presented in detail. The 3D differential transform of a function $q(x, y, z)$ is defined as follows

$$Q(k, h, m) = \frac{1}{k!h!m!} \left[\frac{\partial^{k+h+m} q(x,y,z)}{\partial x^k \partial y^h \partial z^m} \right]_{(0,0,0)} \quad (1)$$

where $q(x, y, z)$ is the original function and $Q(k, h, m)$ is the transformed function. The inverse differential transform of $Q(k, h, m)$ is given by

$$q(x, y, z) = \sum_{k=0}^{\infty} \sum_{h=0}^{\infty} \sum_{m=0}^{\infty} Q(k, h, m) x^k y^h z^m \quad (2)$$

Some of the fundamental theorems on differential transform can be found in [16-21].

3. Strong Form Meshless Implementation of Taylor Series Methods (SMITSM)

In this section, three different basis function formulations based on the DTM are given for 1D and 2D dimensional cases. These methods are named as followings;

1. Strong form meshless implementation of Taylor series method I (SMITSM I),
2. Strong form meshless implementation of Taylor series method II (SMITSM II) and
3. Strong form meshless implementation of Taylor series method III (SMITSM III)

3.1 Strong form meshless implementation of Taylor series method I

One Dimensional Case:

For a function $T(x)$ which has continuous derivatives up to the $(n+1)$ th order, the value of the function at a point $\xi = x$ located in the neighborhood of the point $x = x_i$ can be written through the DTM as follows

$$T(x) = \sum_{k=0}^{\infty} U_i(k)(x - x_i)^k \quad (3)$$

By introducing the two matrices $P(x)$ and U_i , equation (3) can be cast into the following form

$$T(x) = P(x, \xi) U_i \quad (4)$$

where

$$P(x, \xi) = [(x - x_i)^0, (x - x_i)^1, \dots, (x - x_i)^k],$$

$$U_i = [U_i(0), U_i(1), U_i(2), \dots, U_i(k)]^T \quad (5)$$

Elements of the matrix U_i are the unknown variables that can be defined as

$$U_i(k) = \frac{1}{k!} \left[\frac{d^k T_i(x)}{dx^k} \right]_{(x_i)} \quad (6)$$

Depending on the number of unknowns of the matrix U_i , the derivatives of the $T(x)$ (basis function) are obtained. By neglecting the sixth and higher order terms in the DTM expansions, the formulation of the SMITSM I for a 1D problem can be written as follows

$$T(x) = P(x, \xi) U_i$$

$$\frac{dT(x)}{dx} = \frac{dP(x, \xi)}{dx} U_i$$

$$\frac{d^2T(x)}{dx^2} = \frac{d^2P(x, \xi)}{dx^2} U_i$$

$$\frac{d^3T(x)}{dx^3} = \frac{d^3P(x, \xi)}{dx^3} U_i$$

$$\frac{d^4T(x)}{dx^4} = \frac{d^4P(x, \xi)}{dx^4} U_i$$

$$\frac{d^5T(x)}{dx^5} = \frac{d^5P(x, \xi)}{dx^5} U_i \quad (7)$$

Then multiply both sides of the basis function and its derivatives given above by $W(\xi, x)$

$$W(\xi, x) T(x) = W(\xi, x) P(x, \xi) U_i$$

$$W(\xi, x) \frac{dT(x)}{dx} = W(\xi, x) \frac{dP(x, \xi)}{dx} U_i$$

$$W(\xi, x) \frac{d^2T(x)}{dx^2} = W(\xi, x) \frac{d^2P(x, \xi)}{dx^2} U_i$$

$$W(\xi, x) \frac{d^3T(x)}{dx^3} = W(\xi, x) \frac{d^3P(x, \xi)}{dx^3} U_i$$

$$W(\xi, x) \frac{d^4T(x)}{dx^4} = W(\xi, x) \frac{d^4P(x, \xi)}{dx^4} U_i$$

$$W(\xi, x) \frac{d^5T(x)}{dx^5} = W(\xi, x) \frac{d^5P(x, \xi)}{dx^5} U_i$$

(8)

In the compact support of the kernel function $W(\xi, \mathbf{x})$ associated with the point $\mathbf{x} = (x_i, y_i)$ shown in Fig. 1, let there be N_g particles.

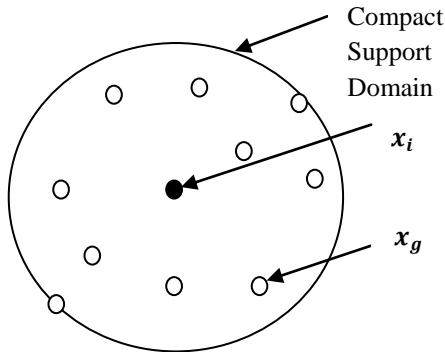


Fig. 1. Distribution of the particles in the compact support of the kernel function $W(\xi, \mathbf{x})$ associated with the point $\mathbf{x} = (x_i, y_i)$

Let's rewrite equation (8) with respect to the compact support domain shown in Fig. 1, evaluate this equation at every particle in the compact support domain of $W(\xi, \mathbf{x})$ and sum each side over these particles, then

$$\begin{aligned} \sum_{g=1}^{N_g} W(x_g, x_i) T(x_g) &= \sum_{g=1}^{N_g} W(x_g, x_i) \mathbf{P}(x_g, x_i) \mathbf{U}_i \\ \sum_{g=1}^{N_g} W(x_g, x_i) T_x(x_g) &= \sum_{g=1}^{N_g} W(x_g, x_i) \mathbf{P}_x(x_g, x_i) \mathbf{U}_i \\ \sum_{g=1}^{N_g} W(x_g, x_i) T_{xx}(x_g) &= \sum_{g=1}^{N_g} W(x_g, x_i) \mathbf{P}_{xx}(x_g, x_i) \mathbf{U}_i \\ \sum_{g=1}^{N_g} W(x_g, x_i) T_{xxx}(x_g) &= \sum_{g=1}^{N_g} W(x_g, x_i) \mathbf{P}_{xxx}(x_g, x_i) \mathbf{U}_i \\ \sum_{g=1}^{N_g} W(x_g, x_i) T_{xxxx}(x_g) &= \sum_{g=1}^{N_g} W(x_g, x_i) \mathbf{P}_{xxxx}(x_g, x_i) \mathbf{U}_i \\ \sum_{g=1}^{N_g} W(x_g, x_i) T_{xxxxx}(x_g) &= \sum_{g=1}^{N_g} W(x_g, x_i) \mathbf{P}_{xxxxx}(x_g, x_i) \mathbf{U}_i \end{aligned} \tag{9}$$

Then, we can solve a set of simultaneous linear algebraic equations given by equation (9) for the unknowns of \mathbf{U}_i for all particles.

Two Dimensional Case:

For a function $T(x, y)$ which has continuous derivatives up to the $(n+1)$ th order, the value of the function at a point

$\xi = (x, y)$ located in the neighborhood of the point $\mathbf{x} = (x_i, y_i)$ can be written through the DTM as follows

$$T(x, y) = \sum_{k=0}^{\infty} \sum_{h=0}^{\infty} U_i(k, h) (x - x_i)^k (y - y_i)^h \tag{10}$$

With the same approach used for 1D case, the following equation can be written

$$T(x, y) = \mathbf{P}(\mathbf{x}, \xi) \mathbf{U}_i \tag{11}$$

where

$$\begin{aligned} \mathbf{P}(\mathbf{x}, \xi) &= [(x - x_i)^0 (y - y_i)^0, (x - x_i)^1 (y - y_i)^0, \\ &\quad (x - x_i)^0 (y - y_i)^1, \dots, (x - x_i)^k (y - y_i)^h], \\ \mathbf{U}_i &= [U_i(0,0), U_i(1,0), U_i(0,1), U_i(2,0), U_i(0,2), \\ &\quad U_i(1,1), \dots, U_i(k, h)]^T \end{aligned} \tag{12}$$

Elements of the matrix \mathbf{U}_i are unknown that can be defined as

$$U_i(k, h) = \frac{1}{k!h!} \left[\frac{\partial^{k+h} T(x,y)}{\partial x^k \partial y^h} \right]_{(x_i, y_i)} \tag{13}$$

By applying the same procedures given for 1D case and neglecting the third and higher order terms in the DTM expansions, the formulation of the SMITSM I for a 2D problem can be written as follows

$$\begin{aligned} \sum_{g=1}^{N_g} W(\xi_g, x_i) T(x_g) &= \sum_{g=1}^{N_g} W(\xi_g, x_i) \mathbf{P}(\xi_g, x_i) \mathbf{U}_i \\ \sum_{g=1}^{N_g} W(\xi_g, x_i) T_x(x_g) &= \sum_{g=1}^{N_g} W(x_g, x_i) \mathbf{P}_x(\xi_g, x_i) \mathbf{U}_i \\ \sum_{g=1}^{N_g} W(\xi_g, x_i) T_y(x_g) &= \sum_{g=1}^{N_g} W(\xi_g, x_i) \mathbf{P}_y(\xi_g, x_i) \mathbf{U}_i \\ \sum_{g=1}^{N_g} W(\xi_g, x_i) T_{xx}(x_g) &= \sum_{g=1}^{N_g} W(\xi_g, x_i) \mathbf{P}_{xx}(\xi_g, x_i) \mathbf{U}_i \\ \sum_{g=1}^{N_g} W(\xi_g, x_i) T_{yy}(x_g) &= \sum_{g=1}^{N_g} W(\xi_g, x_i) \mathbf{P}_{yy}(\xi_g, x_i) \mathbf{U}_i \\ \sum_{g=1}^{N_g} W(\xi_g, x_i) T_{xy}(x_g) &= \sum_{g=1}^{N_g} W(\xi_g, x_i) \mathbf{P}_{xy}(\xi_g, x_i) \mathbf{U}_i \end{aligned} \tag{14}$$

The set of simultaneous linear algebraic equations given in equation (14) can be solved for the unknowns of \mathbf{U}_i for all particles. The formulation for 3D problems can be obtained in a similar fashion as described above.

3.2 Strong form meshless implementation of Taylor series method II

One Dimensional Case:

If we multiply both sides of equation (4) by $W(\xi, x)$, we obtain

$$W(\xi, x)T(x) = W(\xi, x)P(x)U_i \quad (15)$$

Depending on the number of unknowns of the matrix U_i , the derivatives of Equation 3.13 are obtained. By neglecting the sixth and higher order terms in the DTM expansions, the formulation of the SMITSM II for a 1D problem can be written by evaluating equation (15) and its derivatives at every particle in the compact support domain of $W(\xi, x)$ and sum each side over these particles as follows

$$\begin{aligned} \sum_{g=1}^{N_g} W(x_g, x_i) T(x_g) &= \sum_{g=1}^{N_g} W(x_g, x_i) P(x_g, x_i) U_i \\ \sum_{g=1}^{N_g} (W(x_g, x_i) T_x(x_g) + W_x(x_g, x_i) T(x_g)) &= \\ \sum_{g=1}^{N_g} (W(x_g, x_i) P_x(x_g, x_i) + W_x(x_g, x_i) P(x_g, x_i)) U_i & \\ \sum_{g=1}^{N_g} (W(x_g, x_i) T_{xx}(x_g) + 2W_x(x_g, x_i) T_x(x_g) & \\ + W_{xx}(x_g, x_i) T(x_g)) & \\ = \sum_{g=1}^{N_g} (W(x_g, x_i) P_{xx}(x_g, x_i) & \\ + 2W_x(x_g, x_i) P_x(x_g, x_i) & \\ + W_{xx}(x_g, x_i) P(x_g, x_i)) U_i & \\ \sum_{g=1}^{N_g} (W(x_g, x_i) T_{xxx}(x_g) + 3W_x(x_g, x_i) T_{xx}(x_g) & \\ + 3W_{xx}(x_g, x_i) T_x(x_g) & \\ + W_{xxx}(x_g, x_i) T(x_g)) & \\ = \sum_{g=1}^{N_g} (W(x_g, x_i) P_{xxx}(x_g, x_i) & \\ + 3W_x(x_g, x_i) P_{xx}(x_g, x_i) + 3W_{xx}(x_g, x_i) P_x(x_g, x_i) & \\ + W_{xxx}(x_g, x_i) P(x_g, x_i)) U_i & \\ \sum_{g=1}^{N_g} (W(x_g, x_i) T_{xxxx}(x_g) + 4W_x(x_g, x_i) T_{xxx}(x_g) + & \\ 6W_{xx}(x_g, x_i) T_{xx}(x_g) + 4W_{xxx}(x_g, x_i) T_x(x_g) + & \\ W_{xxxx}(x_g, x_i) T(x_g)) = & \\ \sum_{g=1}^{N_g} (W(x_g, x_i) P_{xxxx}(x_g, x_i) + 4W_x(x_g, x_i) P_{xxx}(x_g, x_i) & \\ + 6W_{xx}(x_g, x_i) P_{xx}(x_g, x_i) + 4W_{xxx}(x_g, x_i) P_x(x_g, x_i) & \\ + W_{xxxx}(x_g, x_i) P(x_g, x_i)) U_i & \\ \sum_{g=1}^{N_g} (W(x_g, x_i) T_{xxxxx}(x_g) + 5W_x(x_g, x_i) T_{xxxx}(x_g) + & \\ 10W_{xx}(x_g, x_i) T_{xxx}(x_g) + 10W_{xxx}(x_g, x_i) T_{xx}(x_g) + & \end{aligned}$$

$$\begin{aligned} 5W_{xxxx}(x_g, x_i) T_x(x_g)) + W_{xxxxx}(x_g, x_i) T(x_g)) = & \\ \sum_{g=1}^{N_g} (W(x_g, x_i) P_{xxxxx}(x_g, x_i) + 5W_x(x_g, x_i) P_{xxxx}(x_g, x_i) & \\ + 10W_{xx}(x_g, x_i) P_{xxx}(x_g, x_i) + & \\ 10W_{xxx}(x_g, x_i) P_{xx}(x_g, x_i) + 5W_{xxxx}(x_g, x_i) P_x(x_g, x_i) + & \\ W_{xxxxx}(x_g, x_i) P(x_g, x_i)) U_i & \quad (16) \end{aligned}$$

The set of simultaneous linear algebraic equations given by equation (16) can be solved for the unknowns of U_i for all particles.

Two Dimensional Case:

If we multiply both sides of equation (11) by $W(\xi, \mathbf{x})$, we obtain

$$W(\xi, \mathbf{x})T(x, y) = W(\xi, \mathbf{x})P(\mathbf{x})U_i \quad (17)$$

Depending on the number of unknowns of the matrix U_i , the derivatives of the equation (17) are obtained. By neglecting the third and higher order terms in the DTM expansions, the formulation of the SMITSM II for a 2D problem can be written by evaluating equation (17) and its derivatives at every particle in the compact support domain of $W(\xi, \mathbf{x})$ and sum each side over these particles as follows

$$\begin{aligned} \sum_{g=1}^{N_g} W(\xi_g, \mathbf{x}_i) T(\mathbf{x}_g) &= \sum_{g=1}^{N_g} W(\xi_g, \mathbf{x}_i) P(\xi_g, \mathbf{x}_i) U_i \\ \sum_{g=1}^{N_g} (W(\xi_g, \mathbf{x}_i) T_x(\mathbf{x}_g) + W_x(\xi_g, \mathbf{x}_i) T(\mathbf{x}_g)) & \\ = \sum_{g=1}^{N_g} (W(\xi_g, \mathbf{x}_i) P_x(\xi_g, \mathbf{x}_i) + W_x(\xi_g, \mathbf{x}_i) P(\xi_g, \mathbf{x}_i)) U_i & \\ \sum_{g=1}^{N_g} (W(\xi_g, \mathbf{x}_i) T_y(\mathbf{x}_g) + W_y(\xi_g, \mathbf{x}_i) T(\mathbf{x}_g)) & \\ = \sum_{g=1}^{N_g} (W(\xi_g, \mathbf{x}_i) P_y(\xi_g, \mathbf{x}_i) + W_y(\xi_g, \mathbf{x}_i) P(\xi_g, \mathbf{x}_i)) U_i & \\ \sum_{g=1}^{N_g} (W(\xi_g, \mathbf{x}_i) T_{xx}(\mathbf{x}_g) + 2W_x(\xi_g, \mathbf{x}_i) T_x(\mathbf{x}_g) & \\ + W_{xx}(\xi_g, \mathbf{x}_i) T(\mathbf{x}_g)) & \\ = \sum_{g=1}^{N_g} (W(\xi_g, \mathbf{x}_i) P_{xx}(\xi_g, \mathbf{x}_i) + 2W_x(\xi_g, \mathbf{x}_i) P_x(\xi_g, \mathbf{x}_i) & \\ + W_{xx}(\xi_g, \mathbf{x}_i) P(\xi_g, \mathbf{x}_i)) U_i & \\ \sum_{g=1}^{N_g} (W(\xi_g, \mathbf{x}_i) T_{yy}(\mathbf{x}_g) + 2W_y(\xi_g, \mathbf{x}_i) T_y(\mathbf{x}_g) & \\ + W_{yy}(\xi_g, \mathbf{x}_i) T(\mathbf{x}_g)) & \end{aligned}$$

$$\begin{aligned}
 &= \sum_{g=1}^{N_g} (W(\xi_g, x_i) P_{yy}(\xi_g, x_i) + 2W_y(\xi_g, x_i) P_y(\xi_g, x_i) \\
 &\quad + W_{yy}(\xi_g, x_i) P(\xi_g, x_i)) U_i \\
 &\sum_{g=1}^{N_g} (W(\xi_g, x_i) T_{xy}(x_g) + W_y(\xi_g, x_i) T_x(x_g) + \\
 &W_x(\xi_g, x_i) T_y(x_g) + W_{xy}(\xi_g, x_i) T(x_g)) = \\
 &\sum_{g=1}^{N_g} (W(\xi_g, x_i) P_{xy}(\xi_g, x_i) + W_y(\xi_g, x_i) P_x(\xi_g, x_i) + \\
 &W_x(\xi_g, x_i) P_y(\xi_g, x_i) + W_{xy}(\xi_g, x_i) P(\xi_g, x_i)) U_i \quad (18)
 \end{aligned}$$

3.3 Strong form meshless implementation of Taylor series method III

One Dimensional Case:

If we multiply both sides of equation (4) by $W(\xi, x)$, we obtain

$$W(\xi, x)T(x) = W(\xi, x)P(x)U_i \quad (19)$$

Let's rewrite equation (19) with respect to the compact support domain shown in Fig. 1, evaluate this equation at every particle in the compact support domain of $W(\xi, x)$ and sum each side over these particles, then

$$\sum_{g=1}^{N_g} W(x_g, x_i)T(x_g) = \sum_{g=1}^{N_g} W(x_g, x_i)P(x_g, x_i)U_i \quad (20)$$

Repeating the above procedure regarding the number of terms included in U_i in equation (5) by replacing W with the following

$$\begin{aligned}
 W_x &= \partial W / \partial x, \\
 W_{xx} &= \frac{\partial^2 W}{\partial x^2}, \\
 W_{xxx} &= \frac{\partial^3 W}{\partial x^3}, \\
 W_{xxxx} &= \frac{\partial^4 W}{\partial x^4}, \\
 W_{xxxxx} &= \frac{\partial^5 W}{\partial x^5}
 \end{aligned} \quad (21)$$

and so on. Then, we can solve a set of simultaneous linear algebraic equations for the unknowns of U_i for all particles.

By neglecting the sixth and higher order terms in the DTM expansions, the formulation of the SMITSM III for a 1D problem can be written as follows

$$\begin{aligned}
 \sum_{g=1}^{N_g} W(x_g, x_i)T(x_g) &= \sum_{g=1}^{N_g} W(x_g, x_i)P(x_g, x_i)U_i \\
 \sum_{g=1}^{N_g} W_x(x_g, x_i)T(x_g) &= \sum_{g=1}^{N_g} W_x(x_g, x_i)P(x_g, x_i)U_i \\
 \sum_{g=1}^{N_g} W_{xx}(x_g, x_i)T(x_g) &= \sum_{g=1}^{N_g} W_{xx}(x_g, x_i)P(x_g, x_i)U_i
 \end{aligned}$$

$$\begin{aligned}
 \sum_{g=1}^{N_g} W_{xxx}(x_g, x_i)T(x_g) &= \sum_{g=1}^{N_g} W_{xxx}(x_g, x_i)P(x_g, x_i)U_i \\
 \sum_{g=1}^{N_g} W_{xxxx}(x_g, x_i)T(x_g) &= \sum_{g=1}^{N_g} W_{xxxx}(x_g, x_i)P(x_g, x_i)U_i \\
 \sum_{g=1}^{N_g} W_{xxxxx}(x_g, x_i)T(x_g) &= \sum_{g=1}^{N_g} W_{xxxxx}(x_g, x_i)P(x_g, x_i)U_i
 \end{aligned} \quad (22)$$

where

$$P(x) = [1, (x - x_i)^1, (x - x_i)^2, (x - x_i)^3, (x - x_i)^4, (x - x_i)^5]$$

$$U_i = [U_i(0), U_i(1), U_i(2), U_i(3), U_i(4), U_i(5)]^T \quad (23)$$

The set of simultaneous linear algebraic equations given by equation (22) can be solved for the unknowns of U_i for all particles.

Two Dimensional Case:

If we multiply both sides of equation (11) by $W(\xi, x)$, we obtain

$$W(\xi, x)T(x, y) = W(\xi, x)P(x)U_i \quad (23)$$

Lets rewrite equation (23) with respect to the compact support domain shown in Figure 1, evaluate this equation at every particle in the compact support domain of $W(\xi, x)$ and sum each side over these particles, then

$$\sum_{g=1}^{N_g} W(\xi_g, x_i)T(\xi_g) = \sum_{g=1}^{N_g} W(\xi_g, x_i)P(\xi_g, x_i)U_i \quad (24)$$

Repeating the above procedure regarding the number of terms included in U_i in Equation (12) by replacing W with the following

$$\begin{aligned}
 W_x &= \partial W / \partial x, \\
 W_y &= \partial W / \partial y, \\
 W_{xx} &= \partial^2 W / \partial yx^2 \\
 W_{yy} &= \partial^2 W / \partial y^2, \\
 W_{xy} &= \frac{\partial^2 W}{\partial x \partial y}
 \end{aligned} \quad (25)$$

and so on. By neglecting the third and higher order terms in the DTM expansions, the formulation of the SMITSM III for a 2D problem can be written as follows

$$\sum_{g=1}^{N_g} W(\xi_g, x_i)T(\xi_g) = \sum_{g=1}^{N_g} W(\xi_g, x_i)P(\xi_g, x_i)U_i$$

$$\begin{aligned}
 \sum_{g=1}^{N_g} W_x(\xi_g, x_i) T(\xi_g) &= \sum_{g=1}^{N_g} W_x(\xi_g, x_i) P(\xi_g, x_i) U_i \\
 \sum_{g=1}^{N_g} W_y(\xi_g, x_i) T(\xi_g) &= \sum_{g=1}^{N_g} W_y(\xi_g, x_i) P(\xi_g, x_i) U_i \\
 \sum_{g=1}^{N_g} W_{xx}(\xi_g, x_i) T(\xi_g) &= \sum_{g=1}^{N_g} W_{xx}(\xi_g, x_i) P(\xi_g, x_i) U_i \\
 \sum_{g=1}^{N_g} W_{yy}(\xi_g, x_i) T(\xi_g) &= \sum_{g=1}^{N_g} W_{yy}(\xi_g, x_i) P(\xi_g, x_i) U_i \\
 \sum_{g=1}^{N_g} W_{xy}(\xi_g, x_i) T(\xi_g) &= \sum_{g=1}^{N_g} W_{xy}(\xi_g, x_i) P(\xi_g, x_i) U_i
 \end{aligned}
 \tag{26}$$

where

$$\begin{aligned}
 P(x) &= [1, (x - x_i)^1, (x - x_i)^2, (x - x_i)^3, (x - x_i)^4, \\
 &\quad (x - x_i)^5] \\
 U_i &= [U_i(0), U_i(1), U_i(2), U_i(3), U_i(4), U_i(5)]^T
 \end{aligned}
 \tag{27}$$

The set of simultaneous linear algebraic equations given by equation (26) can be solved for the unknowns of U_i for all particles.

The formulation for 3D problems can be obtained in similar fashions as described above.

4. Numerical Examples

The SMITSM I, II and III are applied to three sample boundary value problems in this section. Since the SMITSM I, II and III and SSPH method depend on TSEs and employ strong form formulations, results of these methods are compared with each other. Although problem types and domains are simple in the following three examples, they are chosen due to the reasons that their analytical solutions can be derived for comparisons and they illustrate the implementation of the SMITSM in a clear way. Nonetheless, the SMITSM I, II and III and SSPH method can be easily applied to any boundary value problem and complex domains in a systematic way. The computer programs that are used to solve the numerical problems are developed by using Matlab.

4.1 1D Nonhomogeneous Boundary Value Problem

Consider the following 1D nonhomogeneous ordinary differential equation

$$\frac{d^2v}{dx^2} = x^3, \quad 0 \leq x \leq 2 \tag{28}$$

The boundary conditions are given by $v(0) = 1$ and $v(2) = 6.6$. The analytical solution of this boundary value problem is given by

$$v(x) = \frac{1}{20}x^5 + 2x + 1 \tag{29}$$

The above boundary value problem is solved by using the SMITSM I, II and III and SSPH method for the particle distributions of 5, 20 and 100 equally spaced particles in the domain $x \in [0,2]$. The following Revised Super Gauss Function in [11] is used as the kernel function since it resulted in the least L_2 error norms in numerical solutions presented in [13]

$$W(x, \xi) = \frac{G}{(h\sqrt{\pi})^\lambda} \begin{cases} (4 - d^2)e^{-d^2} & 0 \leq d \leq 2 \\ 0 & d > 2 \end{cases} \tag{30}$$

where $d = |x - \xi|/h$ is the radius of the support domain which is set to 2, h is the smoothing length, λ is equal to the dimensionality of the space (i.e., $\lambda=1, 2$ or 3) and G is the normalization parameter having the values 1.04823, 1.10081 and 1.18516 for $\lambda = 1, 2$ and 3 , respectively. It is chosen that the smoothing length h equals to the minimum distance Δ between two adjacent particles.

Numerical results obtained by using the SMITSM I, II and III and SSPH method are compared with the analytical solutions, and their convergence and accuracy features are evaluated by using the following global L_2 error norm

$$\|Error\|_2 = \frac{[\sum_{j=1}^m (v_{num}^j - v_{exact}^j)^2]^{1/2}}{[\sum_{j=1}^m (v_{exact}^j)^2]^{1/2}} \tag{31}$$

where v_{num}^j is the value of numerical solution v at the j^{th} node and v_{exact}^j is the value of analytical solution at the j^{th} node. Considering equation (28), we can obtain the following equation by using the DTM technique

$$\begin{aligned}
 (k + 1)(k + 2)V(k + 2) &= F(k), \\
 F(k) &= \frac{1}{k!} \left[\frac{d^k x^3}{dx^k} \right]_{x=x_j}
 \end{aligned}
 \tag{32}$$

By using equation (32), one can solve for the coefficients $V(2), V(3), V(4)$ and $V(5)$ in terms of $F(0), F(1), F(2)$ and $F(3)$ for all particles located in the compact support domain of a particle. The sixth and higher order terms are neglected in derivations since they are equal to zero for this problem.

Following, the expressions for $V(2), V(3), V(4)$ and $V(5)$ for each particle are assembled to obtain global equations, boundary conditions are imposed and then the resulting equation system is solved. Note that $V(0)$ and $V(1)$ are already defined by boundary conditions for particle number 1; thus, there is no unknown for particle number 1 located at $x=0$.

The global L_2 error norms of the solutions of the SMITSM I, II, and III and SSPH method are given in Table 1.to Table 4. where different numbers of particles and terms in expansions are considered. The results in Table 1.to Table 4. are obtained for the parameter values of d and h giving the best accuracy for each method.

In Table 1., it is observed that the SMITSM II, and III and SSPH method give the lowest error for the numerical solution obtained by using 3 terms. The SMITSM I always give the highest error norm when it is compared to other methods.

The SMITSM I cannot provide satisfactory result for the compact support domain radius of 2 by using 5 nodes.,

Table 1.Global L₂ error norm for different number of nodes – 3 term

Meshless Method	Number of Nodes		
	5 Nodes	20 Nodes	100 Nodes
SMITSM I	*	1.4129277	0.15680171
SMITSM II	1.0455434	0.0542322	0.0020706
SMITSM III	1.0455434	0.0542322	0.0020706
SSPH	1.0454434	0.0542322	0.0020706

*There is no solution for the compact support domain radius d=2.

Table 2.Global L₂ error norm for different number of nodes – 4 term

Meshless Method	Number of Nodes		
	5 Nodes	20 Nodes	100 Nodes
SMITSM I	*	0.05299339	0.0020771
SMITSM II	1.0455434	0.0542322	0.0020706
SMITSM III	1.0455434	0.0542322	0.0020706
SSPH	1.0455434	0.0542322	0.0020706

*There is no solution for the compact support domain radius d=2.

In Table 2., it is found that there is no difference between the methods in terms of global L₂ error norm for different number of nodes by using 4 term in the TSE expansion. The SMITSM I cannot provide satisfactory results for the compact support domain radius of 2 by using 5 nodes.

It is observed in Table 3. that the SMITSM I and II always give the lowest global L₂ error norm for different number of nodes by using 5 term in the TSE expansion. The SMITSM I cannot provide satisfactory results for the compact support domain radius of 2 by using 5 nodes.

Table 3.Global L₂ error norm for different number of nodes – 5 term

Meshless Method	Number of Nodes		
	5 Nodes	20 Nodes	100 Nodes
SMITSM I	*	0.0019065	1.6x10 ⁻⁶
SMITSM II	4.5x10 ⁻¹⁴	1.2x10 ⁻¹¹	2.3x10 ⁻⁹
SMITSM III	3.1x10 ⁻¹⁴	4.9x10 ⁻¹³	3.6x10 ⁻¹²
SSPH	0.1258686 **	0.0001205 **	3.6x10 ⁻⁸

*There is no solution for the compact support domain radius d=2

**The compact support domain radius d is chosen as 4, because d=2 results in large L₂ error norms or no solution with the current smoothing length assumption. It is clear that, even with the same number of terms, solutions of the SMITSM II and III agree very well with the analytical solution; however, those obtained by using the SSPH method and SMITSM I differ noticeably from the analytical solution especially for 5 nodes and 5 terms in the TSEs.

It is observed in Table 4 that the SMITSM II and III agree very well with the analytical solution. The SSPH method cannot provide solution by using 5 nodes in the problem domain when it uses 6 terms in TSE. The SMITSM

I cannot provide satisfactory result for the compact support domain radius of 2 by using 5 nodes.

Table 4.Global L₂ error norm for different number of nodes – 6 term

Meshless Method	Number of Nodes		
	5 Nodes	20 Nodes	100 Nodes
SMITSM I	*	2.4x10 ⁻¹³	3.9x10 ⁻¹²
SMITSM II	7.9x10 ⁻¹⁴	1.4x10 ⁻¹¹	3.6x10 ⁻⁹
SMITSM III	7.8x10 ⁻¹⁴	3.3x10 ⁻¹³	3.6x10 ⁻¹²
SSPH	**	1.3x10 ⁻⁹ ***	2.6x10 ⁻⁹ ***

*There is no solution for the compact support d=2

** At least 6 nodes are needed to solve the problem.

*** The compact support domain radius d is used as 5 because d=2, 3 and 4 result in large L₂ error norms with the current smoothing length assumption. Regarding to the results obtained by using 6 terms in the TSEs, the SMITSM I, II and III give the lowest L₂ error norms.

4.2 Homogeneous Laplace Equation in 2D

The Laplace equation in 2D is solved by using the SMITSM I, II and III and SSPH method in the domain shown in Fig. 2. The governing differential equation and essential boundary conditions are given by

$$\frac{\partial^2 T}{\partial x^2} + \frac{\partial^2 T}{\partial y^2} = 0, \quad T_1 = T_3 = T_4 = 0 \text{ } ^\circ\text{C}, T_2 = 100 \text{ } ^\circ\text{C} \quad (33)$$

where T is the temperature and T_i denote the prescribed boundary temperatures.

The analytical solution of the above boundary value problem is given by

$$\frac{T(x,y)}{T_2} = \sum_{n=1}^{\infty} \frac{2[1-(-1)^n]}{n\pi} \sin\left(\frac{n\pi x}{a}\right) \frac{\sinh\left(\frac{n\pi y}{a}\right)}{\sinh\left(\frac{n\pi b}{a}\right)} \quad (34)$$

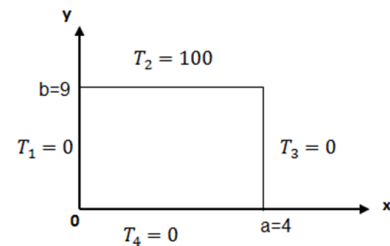


Fig. 2. Problem domain and boundary conditions

When solving this problem, equally spaced 50, 171 and 629 particles are considered in the domain. The smoothing length h is equal to the minimum distance between two adjacent particles (i.e., h = Δ). The following Revised Super Gauss Function in [11] is used as the kernel function

$$W(d) = \frac{G}{(h\sqrt{\pi})^\lambda} \begin{cases} (16 - d^2)e^{-d^2} & 0 \leq d \leq 4 \\ 0 & d > 4 \end{cases} \quad (35)$$

where d = |x - ξ|/h is set to 4, λ = 2 and G has the same value as in Section 4.1.

Convergence and accuracy of the SMITSM I, II and III and SSPH method are calculated by using the following global L₂ error norm

$$\|Error\|_2 = \frac{[\sum_{j=1}^m \{(u_{num}^j - u_{exact}^j)^2 + (v_{num}^j - v_{exact}^j)^2\}]^{1/2}}{[\sum_{j=1}^m \{(u_{exact}^j)^2 + (v_{exact}^j)^2\}]^{1/2}} \quad (36)$$

where u_{num}^j and v_{num}^j are respectively the values of numerical solutions of u and v at the j^{th} node, and u_{exact}^j and v_{exact}^j are respectively the values of analytical solutions of u and v at the j^{th} node.

From equation (33), we can obtain the following recursive equation by using the DTM technique

$$(k + 1)(k + 2)T(k + 2, m) + (m + 1)(m + 2)T(k, m + 2) = 0 \quad (37)$$

The vectors P and U_i can be rearranged as follows

$$P(x, \xi) = [1, (x - x_i)^1, (y - y_i)^1, (x - x_i)^2, (y - y_i)^2, (x - x_i)^1(y - y_i)^1,$$

$$(x - x_i)^3 - 3.(x - x_i)^1(y - y_i)^2, (x - x_i)^2(y - y_i)^1 - (1/3)((y - y_i)^2),$$

$$(x - x_i)^3(y - y_i)^1 - (x - x_i)^1(y - y_i)^3, (x - x_i)^4 - 6.(x - x_i)^2(y - y_i)^2 + (y - y_i)^4$$

$$(x - x_i)^5 - 10.(x - x_i)^3(y - y_i)^2 + 5.(x - x_i)^1(y - y_i)^4$$

$$(x - x_i)^4(y - y_i)^1 - 2.(x - x_i)^2(y - y_i)^3 + (1/5).(y - y_i)^5]$$

$$U_i = [U_i(0,0), U_i(1,0), U_i(0,1), U_i(2,0), U_i(1,1), U_i(3,0),$$

$$U_i(3,1), U_i(4,0), U_i(5,0), U_i(4,1)]^T \quad (38)$$

Following, above nodal equations are assembled to obtain the global equations; then, boundary conditions are imposed and the resulting equation system is solved. To evaluate the performance, numerical solutions are obtained for 6 terms for the SMITSM I, II and III and SSPH method. Numerical solutions obtained by using 6 terms in the associated expansions and 50, 171 and 629 nodes are presented in Fig. 3, 4 and 5, respectively.

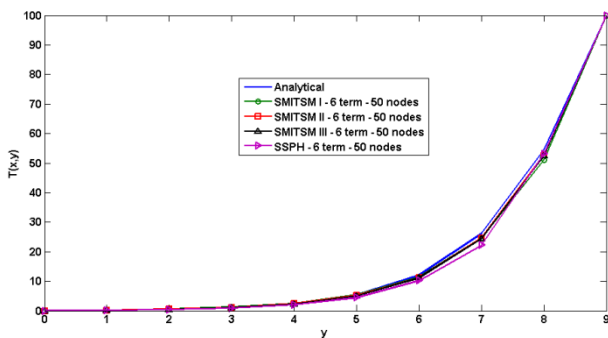


Fig. 3. Temperatures along the y-axis ($x=2$) computed by the SMITSM, SSPH method and analytical solution where equally spaced 50 nodes are used

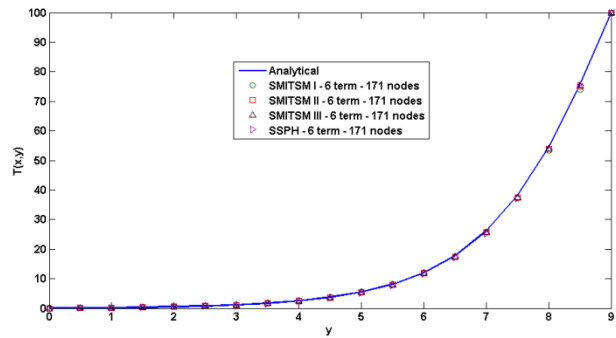


Fig. 4. Temperatures along the y-axis ($x=2$) computed by the SMITSM, SSPH method and analytical solution where equally spaced 171 nodes are used

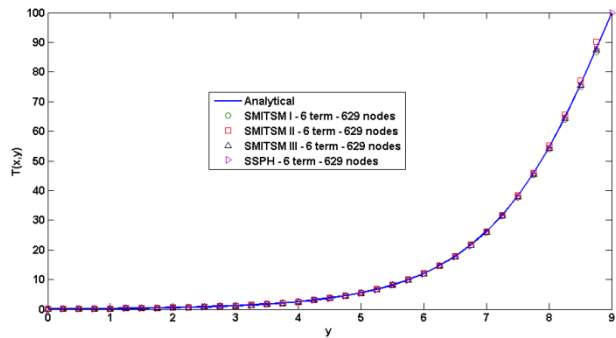


Fig. 5. Temperatures along the y-axis ($x=2$) computed by the SMITSM, SSPH method and analytical solution where equally spaced 629 nodes are used

It is observed in Fig. 3, 4 and 5 that accuracy of the SMITSM I, II and III are better than that of the SSPH method and all studied methods show convergence as the number of nodes is increased.

The global L_2 error norms obtained by the SMITSM I, II and III and SSPH method are given in Table 5. It is clear that the L_2 error norms of the results of the SMITSM I, II and III are much lower than those of the SSPH method provided that the same number of terms in the associated expansions are employed for both methods.

By using the same number of terms, the SMITSM II always gives the lowest global L_2 error norm when comparing with the other methods. The SSPH method always gives the highest L_2 error norms for different number of nodes in the problem domain. Numerical results also show that lower L_2 error norms can be obtained for all methods as the number of particles distributed in the problem domain is increased.

Table 5. Global L_2 error norm for different number of nodes

Meshless Method	Number of Nodes		
	50 Nodes	171 Nodes	629 Nodes
SMITSM I	3.7853	2.1886	1.2718
SMITSM II	3.2134	1.6750	0.9927
SMITSM III	3.7313	1.9813	1.0541
SSPH	8.4205	4.3004	2.3956

4.3 Nonhomogeneous Laplace Equation in 2D

Nonhomogeneous Laplace equation in 2D is solved by using the SMITSM I, II and III and SSPH method in the domain shown in Fig. 6. The governing differential equation and essential boundary conditions are given by

$$\frac{\partial^2 T}{\partial x^2} + \frac{\partial^2 T}{\partial y^2} = -2\text{Sin}x\text{Cos}y, T_1 = 0 \text{ }^\circ\text{C}, T_2 = \bar{T}_2 \text{ }^\circ\text{C},$$

$$T_3 = \bar{T}_3 \text{ }^\circ\text{C}, \frac{\partial T_4(x,0)}{\partial y} = 0(38)$$

where T is the temperature and T_i denote the prescribed boundary temperatures.

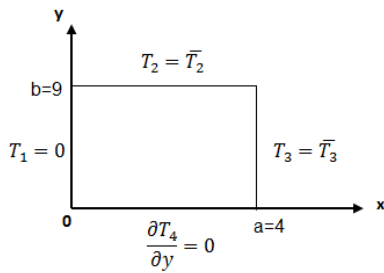


Fig. 6. Problem domain and boundary conditions

The analytical solution of the above boundary value problem is given by

$$T(x, y) = \text{Sin}x\text{Cos}y \quad (39)$$

The solution of this problem is obtained by using the same node distributions, kernel function and kernel function parameters as given in Section 4.2. Convergence and accuracy properties of the SMITSM I, II and III and SSPH method are examined by using the global L_2 error norm given by equation (36).

From equation (38), we can obtain the following recursive equation by using the DTM technique

$$(k + 1)(k + 2)T(k + 2, m) + (m + 1)(m + 2)T(k, m + 2) = -2 \frac{1}{k!m!} \left[\frac{\partial^{k+m} \text{Sin}x\text{Cos}y}{\partial x^k \partial y^m} \right]_{(x,y)} \quad (40)$$

Then, the vectors \mathbf{P} and \mathbf{U}_i can be written as follows

$$\mathbf{P}(x, \xi) = [1, (x - x_i)^1, (y - y_i)^1, (x - x_i)^2, (y - y_i)^2, (x - x_i)^1(y - y_i)^1]$$

$$\mathbf{U}_i = [U_i(0,0), U_i(1,0), U_i(0,1), U_i(2,0), U_i(0,2), U_i(1,1)]^T \quad (41)$$

The numerical solutions obtained by using 6 terms in the associated expansions and 50, 171 and 629 nodes are presented in Fig. 7 to Fig. 12.

In Fig. 7 to Fig. 9, it is observed that the L_2 error norms of the SMITSM II and III with the variation of the radius of the support domain (where $h=\Delta$) are much lower than those of the SMITSM I and the SSPH method provided that the same number of terms are employed in the associated TSEs for both methods.

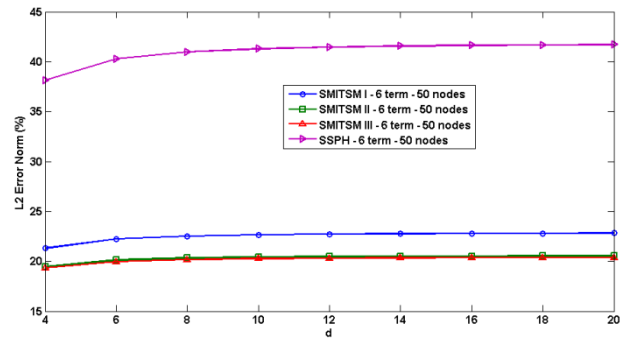


Fig. 7. The global L_2 error norms as the radius of the support domain ($h=\Delta$) varies, where equally spaced 50 nodes are used

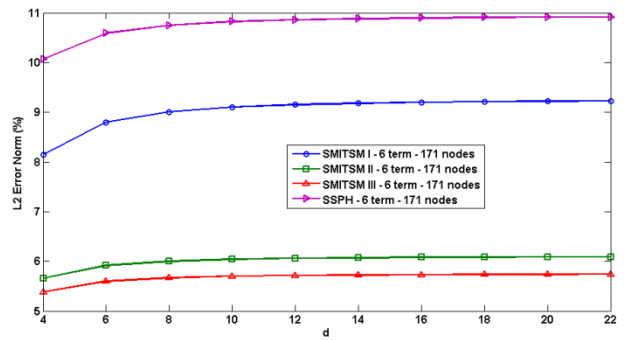


Fig. 8. The global L_2 error norms as the radius of the support domain ($h=\Delta$) varies, where equally spaced 171 nodes are used

It is observed in Fig. 10 to Fig. 12 that accuracy of the SMITSM II and III is better than that of the SMITSM I and SSPH method as the smoothing length parameter varies provided that the same number of terms are employed in the associated TSEs for both methods.

Numerical results imply that the global L_2 error norm of numerical solutions increase as smoothing length parameter increases for all methods. It is observed that the SSPH method is stable for $h=1.8\Delta$ and node distribution of 171 nodes; however, the SMITSM I, II and III are stable even for $h=2\Delta$ as can be seen in Fig. 10.

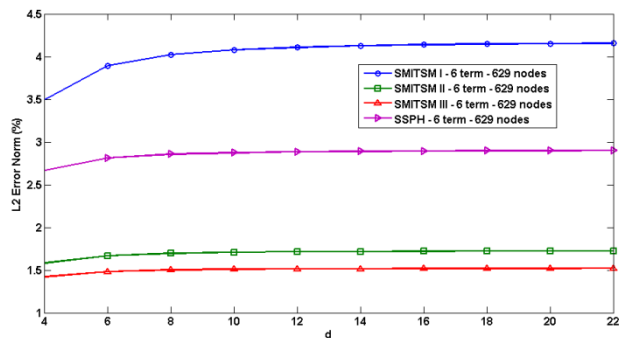


Fig. 9. The global L_2 error norms as the radius of the support domain ($h=\Delta$) varies, where equally spaced 629 nodes are used

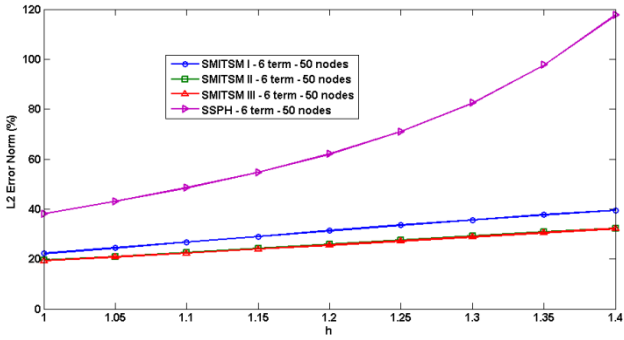


Fig. 10. The global L_2 error norm as the smoothing length varies, where equally spaced 50 nodes are used.

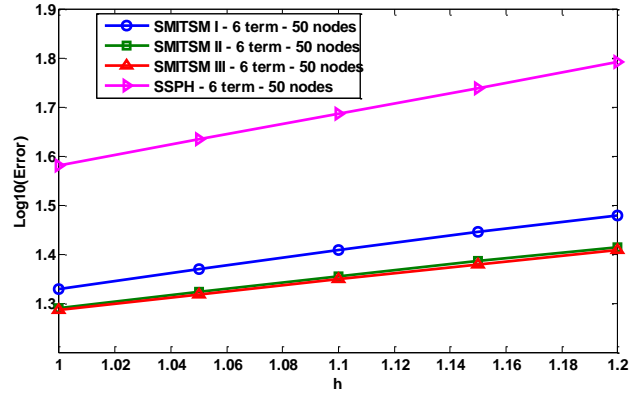


Fig. 13. The convergence rate of the error norm, where equally spaced 50 nodes are used

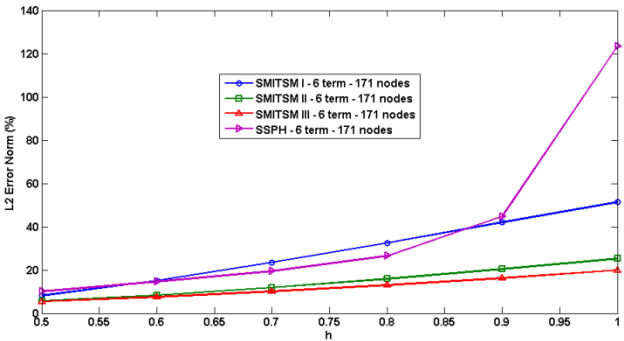


Fig. 11. The global L_2 error norms as the smoothing length varies, where equally spaced 171 nodes are used

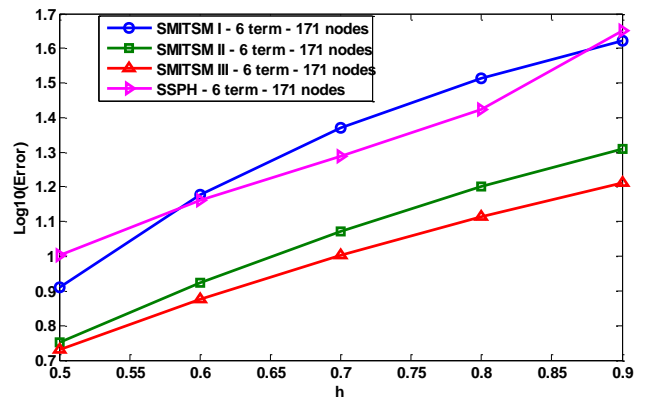


Fig. 14. The convergence rate of error norm, where equally spaced 171 nodes are used

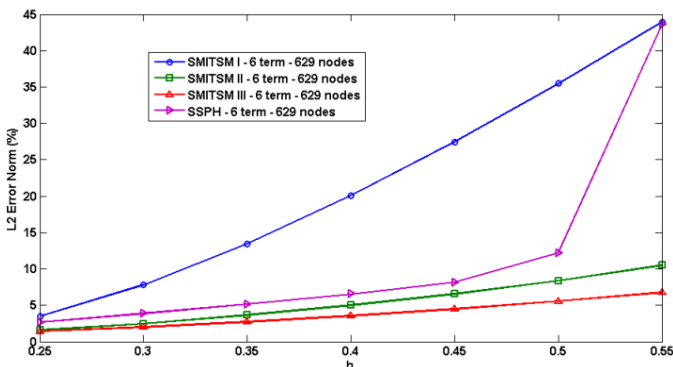


Fig. 12. The global L_2 error norms as the smoothing length varies, where equally spaced 629 nodes are used

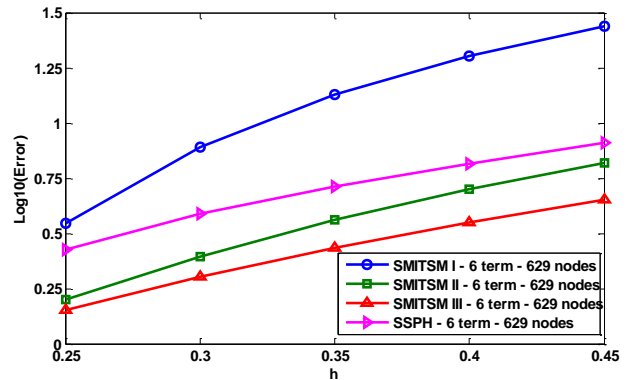


Fig. 15. The convergence rate of the error norm, where equally spaced 629 nodes are used

It is also observed that the SSPH method is stable for $h=2\Delta$ and node distribution of 629 nodes; however, the SMITSM II and III are stable even for $h=2.2\Delta$ as can be seen in Fig. 12

Except for 629 nodes in the problem domain, the SSPH method always gives the highest global L_2 error norm; on the other hand, for 629 nodes, the SMITSM I gives the highest global L_2 error norm.

To find the rate of convergence of numerical solutions with respect to the distance between adjacent particles, the global L_2 error norm is used. The convergence rates of the error norm are presented in Fig. 13 to Fig. 15.

It is observed that the convergence rate of the SSPH method is higher than the other methods for 50 nodes. And also SMITSM I, II and III has nearly the same convergence rate of error norm for 50 nodes in the problem domain.

For 171 and 629 nodes, SMITSM I has the highest convergence rate or error norm. The converge rate of SMITSM II, III and SSPH methods are nearly the same.

5. Conclusion

We presented a new meshless approach called the SMITSM I, II and III by using the TSEs and utilizing the DTM technique. It is observed that the SMITSM II and III yields more accurate results than the SSPH method especially in the existence of nonsmooth nonhomogenous terms. The SMITSM I, II and III does not involve any approximation and its formulations are exact except for the truncations in the TSEs. In addition, as the number of terms in the TSEs and/or nodes in numerical examples are increased, its L_2 error norm decreases that is the evidence of the convergence of the SMITSM I, II and III.

Note that CPU times of the SMITSM I, II and III in solving numerical examples are much larger than those of the SSPH method. Nonetheless, the CPU time and memory requirement of the SMITSM I, II and III can be reduced by utilizing the block form of the associated equation systems, which is not investigated in this paper and will be the subject of future studies.

Even though strong form of the MITSM is considered in this paper, the same approach can easily be applied to weak formulations that leads to Weak Form Meshless Implementation of Taylor Series Method (WMITSM), that will be the subject of future studies as well.

Acknowledgements

The author thanks to anonymous reviewers for their helpful suggestions. The author also thanks to PhD advisor Ata Mugan for his endless support and encouragement.

References

- [1] LB Lucy, A numerical approach to the testing of the fission hypothesis, *Astron J*, Vol. 82, pp. 1013–1024, 1987.
- [2] JK Chen, JE Beraun, CJ Jin, An improvement for tensile instability in smoothed particle hydrodynamics, *Comput Mech.*, Vol. 23, pp. 279–287, 1999.
- [3] JK Chen, JE Beraun, CJ Jin, Completeness of corrective smoothed particle method for linear elastodynamics, *Comput Mech.* Vol. 24, pp. 273–285, 1999.
- [4] WK Liu, S Jun, YF Zhang, Reproducing kernel particle methods, *Int J Num Meth Fluids*, Vol. 20, pp. 1081–1106, 1996.
- [5] WK Liu, S Jun, S Li, J Adee, T Belytschko, Reproducing kernel particle methods for structural dynamics, *Int J Num Meth Eng.*, Vol. 38 pp. 1655–1679, 1995.
- [6] JS Chen, C Pan, CT Wu, WK Liu, Reproducing kernel particle methods for large deformation analysis of non-linear structures, *Comput Method Appl Mech Eng.*, Vol. 139, pp. 195–227, 1996.
- [7] GM Zhang, RC Batra, Modified smoothed particle hydrodynamics method and its application to transient problems, *Comput Mech.*, Vol. 34, pp. 137–146, 2004.
- [8] RC Batra, GM Zhang, Analysis of adiabatic shear bands in elasto-thermo-viscoplastic materials by modified smoothed particle hydrodynamics (MSPH) method, *J Comput Phys.*, Vol. 20, pp. 172–190, 2004.
- [9] GM Zhang, RC Batra, Wave propagation in functionally graded materials by modified smoothed particle hydrodynamics (MSPH) method, *J Comput Phys.*, Vol. 222, pp. 374–390, 2007.
- [10] RC Batra, GM Zhang, Search algorithm, and simulation of elastodynamic crack propagation by modified smoothed particle hydrodynamics (MSPH) method, *Comput Mech.*, Vol. 40, pp. 531–546, 2007.
- [11] GM Zhang, RC Batra, Symmetric smoothed particle hydrodynamics (SSPH) method and its application to elastic problems, *Comput Mech.*, Vol. 43, pp. 321–340, 2009.
- [12] RC Batra, GM Zhang, SSPH basis functions for meshless methods, and comparison of solutions with strong and weak formulations, *Comput Mech.* Vol. 41, pp. 527–545, 2008.
- [13] A Karamanli, A Mugan, Solutions of two-dimensional heat transfer problems by using symmetric smoothed particle hydrodynamics method, *Journal of Applied and Computational Mathematics*, Vol. 1, pp. 1–6, 2012.
- [14] A Karamanli, A Mugan, Strong form meshless implementation of Taylor series method, *Appl. Math. Comput.*, Vol. 219, pp. 9069–9080, 2013.
- [15] C Bervillier, Status of the differential transformation method, *Appl. Math. Comput.*, Vol. 218, pp. 10158–10170, 2012.
- [16] H Liu, Y Song, Differential transform method applied to high index differential-algebraic equations, *App Math Comput.*, Vol. 184, pp. 748–753, 2007.
- [17] F Ayaz, Solutions of the system of differential equations by differential transform method, *App Math Comput.* Vol. 147, pp. 547–567, 2004.
- [18] HS Yalcin, A Arikoglu, I Ozkol, Free vibration analysis of circular plates by differential transform method, *App Math Comput.*, Vol. 212, pp. 377–386, 2009.
- [19] A Arikoglu, I Ozkol, Solution of differential-difference equations by using differential transform method, *App Math Comput.*, Vol. 181, pp. 153–162, 2006.
- [20] A Arikoglu, I Ozkol, Solution of difference equations by using differential transform method, *App Math Comput.*, Vol. 174, pp. 1216–1228, 2006.
- [21] A Arikoglu, I Ozkol, Solution of boundary value problems for integro differential equations by using differential transform method, *App Math Comput.* Vol. 168, pp. 1145–1158, 2005.

Flow Visualization of Sloshing in an Accelerated Two-Dimensional Rectangular Tank

Gurhan Sahin, Seyfettin Bayraktar[‡]

Department of Naval Architecture & Marine Engineering, Faculty of Naval Architecture & Maritime,
Yildiz Technical University, 34349 Istanbul, Turkey

(sahin.gurhan@gmail.com, sbay@yildiz.edu.tr)

[‡]Corresponding Author; Seyfettin Bayraktar, Yildiz Technical University, Department of Naval Architecture & Marine Engineering, Faculty of Naval Architecture & Maritime, 34349 Istanbul, Turkey, Tel: +90 212 383 7070,

sbay@yildiz.edu.tr

Received: 31.07.2015 Accepted: 11.09.2015

Abstract-In the present paper, sloshing in a Two-Dimensional (2D) square liquid tank subjected to horizontal excitation is investigated by means of Computational Fluid Dynamics (CFD) technique. The tank with/without the vertical and horizontal baffles located at each side walls of the tank is moved on positive (+) x-axis for the excitation of 4.5 m²/s for each case study. After series of simulations results obtained for each tank configuration are compared and flow is visualized for the tanks that are 50% filled with the fresh water.

Keywords: Computational fluid dynamics (CFD), turbulence, sloshing, fluid, accelerated tank

1. Introduction

Sloshing is an important engineering problem. It may cause large deformations to wall and supporting structures in partially filled tanks. According to the classification societies' guidance sloshing may be defined as violent behavior of the liquid contents in tanks [1]. The phenomenon can be seen in many industries including automotive, aerospace, motorcycle, shipbuilding and maritime from the sloshing oscillations in aircrafts or space-crafts to storage tanks of ocean-going ships [2, 3].

Different wave conditions in partially filled tanks, uncontrolled loading/unloading processes, structural frequencies, shape and position of the tank, sources of the motions, filling levels inside the tanks, density of the fluid, etc. may cause sloshing. The tanks may be rectangular, prismatic, tapered, spherical and cylindrical. The carried liquids may be oil, liquefied gas, water, molasses and caustic soda [4]. All these above parameters show how the sloshing is complex and difficult to analyze. As stated by Rudman and Cleary [5] sloshing affects ship stability and therefore, great attention must be paid during not also loading and/or unloading period but also transportation. Due to demand of sloshing analysis for building large Liquefied Natural Gases (LNG) carriers and LNG platforms classification societies

publish rules and guidance on this issue. For example, Bureau Veritas [1] and Det Norske Veritas [6] show the importance and specify the basic requirements for approval of LNG carriers and floating structures as well as provide necessary methodology to assess the sloshing loads and how to use these methodologies. One may ask why tanks are left partially-filled. The reason is that partial fillings in LNG carriers are a consequence of boil-off of gas during operations [4]. Up to now many experimental and numerical works have been performed. Krata [7] presented the results of an experimental and numerical works of a tank filled partially with the water. The pressure was measured while the tank was oscillated with the amplitude of 18°, 30°, and 40° which reflects the worst heavy sea conditions. Results showed that the measured pressure consists of non-impulsive dynamic pressure and impulsive (impact) pressure. The first one varies slowly due to the global movement of the liquid in the tank while the second lasts shortly and due to the hydraulic jump. An improved volume of fluid (VOF) model was developed by Wemmenhove et al. [8] and the numerical results were compared by a 1:10 model test. Although no any details on computational approach were given it was claimed that both numerical and experimental results were in a good agreement. Hou et al. [9] imposed external single and multiple excitations to the tank and analyzed the sloshing by CFD technique. It was revealed that the sloshing effects

increased when the numbers of coupled excitations were added. Shoji and Munakata [10] tried to analyze the sloshing due to an earthquake by means of Fluid-Structure Interaction (FSI) and their results cleared that the current potential theories does not agree so much with the FSI analyses. Lots of methods have been employed to analyze the sloshing characteristics such as quasi-static method, hydrodynamics method, experimental method, equivalent mechanical method and computer simulation. Interested readers may find detailed knowledge in the work of Xue-Lian et al. [11]. Each technique has some advantages and disadvantages and among them experimental and computational techniques take more interests.

One of the fuel tank design objectives is to effectively reduce noise level caused by fluid motion inside the tank by designing baffles and separators to control the sloshing. In addition, alternate materials and manufacturing processes are evaluated for fuel tank design in order to reduce weight and cost and to provide structural integrity for higher structural performance. Sloshing in the tank may be controlled by incorporating baffles, and the effectiveness highly depends on the shape, the location, and the number of baffles inside a tank.

In the present paper, one of the test cases of Akyildiz and Celebi [12] and Javanshir et al. [13] is inspired where a rectangular tank was separated into mainly three regions by means of a vertical and two horizontal baffles. In addition to these types of configurations, a new one is introduced in the present paper and analyzed by means of CFD. The horizontal baffles that connected to the left and rights walls of the tanks are raised 15° upwards.

2. Figures and Tables

It is obvious that sloshing occurs due to motion of fluid inside partially filled moving tank. As a passive control method baffles can be used to reduce the severe effects of sloshing. The following case studies simulate sloshing in a partially filled rigid tanks with and without the baffles and report the results for each configurations.

2.1. Tank Configurations

Rectangular tank with 250^{mm}x250^{mm} dimensions are considered to evaluate the performance of sloshing. The tanks with three baffle configurations are filled 50% with fresh water. The dimensions of the tank and baffles are showed in Fig.1. As shown in Fig.1a the first tank do not have any baffles while the second type tank has two horizontal baffles which are parallel to the bottom and a vertical baffle is in the middle of bottom (Fig.1b). Horizontal baffles of third type are angled 15° upward while the vertical baffle is kept constant in the middle of the bottom (Fig.1c). All type of tanks are investigated according to below assumptions:

- Tanks are moving with 4.5 m/s² acceleration in +x direction (in 0-2 s)

- Tanks are moving with 4.5 m/s² acceleration in -x direction (in 2-4 s)
- Tanks are moving with 4.5 m/s² acceleration in +x direction (in 4-6 s)

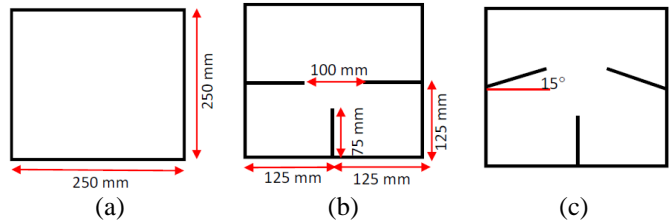


Fig. 1. Tank configurations, a) type-1, b) Type-2, c) Type-3

2.2. Mesh Structure

Number of mesh elements, aspect ratios and skewness that show quality of the mesh structure is summarized in Table.1.

Table 1. Mesh information of each configuration

	Number of elements	Maximum aspect ratio	Maximum skewness
Type-1 tank	50690	1.2896	0.410
Type-2 tank	65528	1.9586	0.573
Type-3 tank	65302	1.8882	0.622

As shown in Fig.2, different mesh elements are used for each tank configuration. Only quadrilateral elements are used for Type-1 tank while hybrid elements (quadrilateral and dominantly triangles) are preferred for Type-2 and Type-3 tanks.

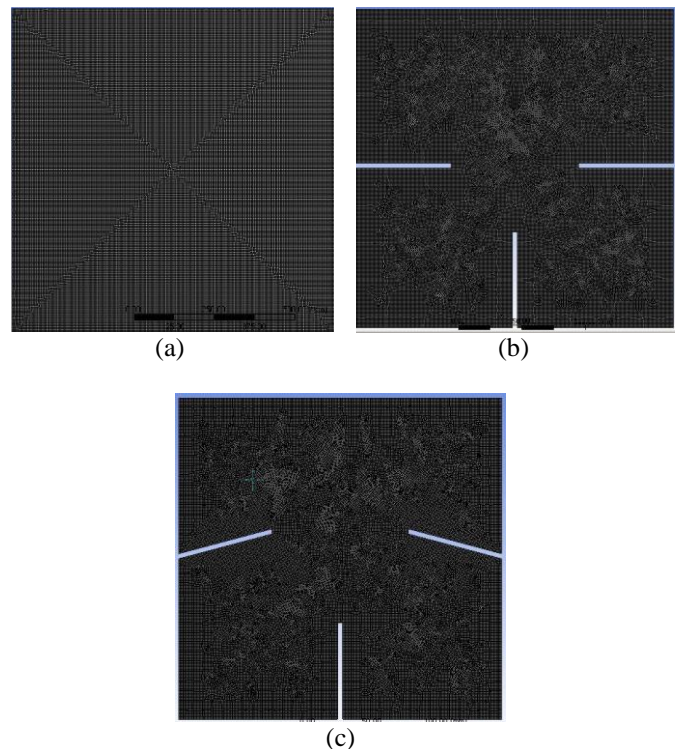


Fig. 2. Mesh structure of a) Type-1, b) Type-2, c) Type-3

3. Mathematical Model

The equations used to simulate the sloshing are the continuity (Eq.1), Navier-Stokes (Eq.2) and VOF equations. These are given in general form as follows:

$$\nabla \vec{V} = 0 \tag{1}$$

$$\frac{D\vec{V}}{Dt} + -\frac{1}{\rho} [\nabla p - \mu(\nabla^2 \vec{V})] + \vec{F}_B \tag{2}$$

The momentum equation is dependent on the volume fractions of all phases and given in Eq.3

$$\frac{\partial u}{\partial t} + (\vec{V} \cdot \nabla) \vec{V} = -\frac{1}{\rho} (\nabla p - \mu(\nabla^2 \vec{V})) + F_B + F_V \tag{3}$$

where \vec{V} is the fluid velocity relative to tank, p is pressure; ρ is fluid density and μ is viscosity. F_B and F_V state body force and virtual body force induced by the motion of tank.

As stated in detail by Nema [14] there are several techniques such as

- Moving grid or Lagrangian approach (capturing),
- Fixed grid or Eulerian approach (tracking),
- Combined method of Langrangian and Eulerian

for tracking immiscible interfaces. In the present study VOF, a part of Eulerian approach, has been used. The VOF model assumes that there is no any interaction between all the fluid phases (air and water here). For each control volume, the volume fraction of the phase in the cell will be introduced and the volume fraction of all the phases sums to unity. If α_b represent the both fluid`s volume fraction in the cell, then the following three conditions are possible:

- $\alpha_b=0$: Shows the cell is empty (no fluid of b type is present)
- $\alpha_b=1$: Shows the cell is full (only b type fluid is present)
- $0 < \alpha_b < 1$: Shows the cell contain the interface between the both fluid and one or more other type of fluid.

Equation of volume fraction (VOF) for the both phase is given in Eq.4.

$$\frac{1}{\rho} \left[\frac{\partial}{\partial t} (\alpha_b \rho_b) \right] + \vec{\nabla} \cdot (\alpha_b \rho_b \vec{V}_b) = s_{\alpha_b} + \sum (\dot{m}_{ab} - \dot{m}_{ba}) \tag{4}$$

where \dot{m}_{ab} , \dot{m}_{ba} and s_{ab} is the mass transfer from a to b phase, mass transfer from b to a phase and source term which permits the use of cavitation model. For n phases:

$$\sum_{b=1}^n \alpha_b = 1 \tag{5}$$

Following equation is used to calculate physical parameters in the 2-phase flow for a and b:

$$\begin{aligned} \rho &= \alpha \rho_b + (1 - \alpha) \rho_a \\ \mu &= \alpha \mu_b + (1 - \alpha) \mu_a \end{aligned} \tag{6}$$

Where α is defined as 1 for water and 0 for air.

As turbulence model, standard k- ϵ is selected that requires the solution of k, turbulent kinetic energy (Eq.7) and ϵ , its dissipation rate (Eq.8).

$$\frac{\partial k}{\partial t} + \frac{(ku_j)}{\partial x_j} = \frac{\partial}{\partial x_j} \left[\left(\nu + \frac{\nu_t}{\sigma_k} \right) \frac{\partial k}{\partial x_j} \right] + P_k - \epsilon \tag{7}$$

$$\frac{\partial \epsilon}{\partial t} + \frac{\partial(\epsilon u_j)}{\partial x_j} = \frac{\partial}{\partial x_j} \left[\left(\nu + \frac{\nu_t}{\sigma_\epsilon} \right) \frac{\partial \epsilon}{\partial x_j} \right] + C_{\epsilon 1} P_K \frac{\epsilon}{k} - C_{\epsilon 2} \frac{\epsilon^2}{k} \tag{8}$$

where P_K is the production of kinetic energy. Value of each coefficient seen in the equations are given in Table 2.

Table 2. Value of coefficients.

$C_{\epsilon 1}$	$C_{\epsilon 2}$	C_μ	σ_k	σ_ϵ
1.44	1.92	0.09	1.0	1.3

It is assumed that there is no slip on tank sides, bottom and top walls. The related equations are solved for time step of 0.01 second for all cases. Recommendations of Javanshir et al. [13] are followed initially. The model was validated by theory [15] and then baffles that are parallels and angled to the bottom of the tanks are used to reduce liquid sloshing.

3.1. Linear Acceleration

Initially, the tank is kept at rest and it is started to move along positive (+) x-direction with constant acceleration of 4.5 m/s². The liquid is deviated from equilibrium state and then moved and clashed with the wall of the tank. After that water is in stable condition at a certain angle. Based on the theory, the free surface of liquid must be perpendicular to the pressure gradient and is thus tilted at a downward angle (θ) that is given in Eq.9 [15]:

$$\theta = \text{Arc tan} \left(\frac{a_x}{a_y + \vec{g}} \right) \tag{9}$$

where \vec{g} , a_x and a_y is the gravitational acceleration (in y-direction), acceleration in x-direction and finally acceleration in y-direction, respectively. Theoretically, θ is found as to be 24.64°. This value is validated by the present CFD study as shown in Fig.3.

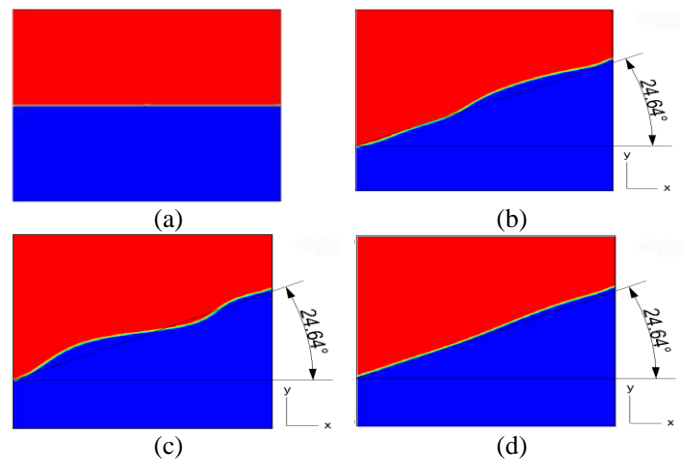


Fig. 3. Sloshing in a rectangular tank without barrels under linear acceleration of 4.5 m/s^2 in the (+) x-direction during a) $t=0$, b) $t=2$ seconds, c) $t=5.5$ seconds, d) $t=10$ seconds

4. Results and Discussion

Fig.4 depicts the position of the free surface under the excitation for different configurations at various time from $T=1$ second to $T=6$ seconds. Since flow is excited towards the (+)x direction at the beginning the water starts to move into that direction, impact on the right wall and then rises. With the gained energy it changes its direction and impacts on the left wall of the tank, then overturns and generates overturning waves (Fig.4a).

In the case of Type-2 tank the fluid (water) cannot rise so much. However, due to the presence of an obstructing object (horizontal baffle) it is disturbed and waves occurred

on top of the baffle. As time goes by some bubbles occurred in the waves (Fig.4b) that play a role to damp the peak pressures of impact because the bubbles reduce the density of the fluid (water) and therefore, damps the pressure effects, [16]. In the present study, no any bubbles are seen around the corner of the tank ceiling but at the corner of the baffles.

It is not seen any wave impact on the side walls when the Type-3 tank is taken into account (Fig.4c). Fluid barely get out of the region created by raised horizontal baffles and could not reach to the side walls at the beginning. After a duration only small-sized waves occurred on the top of the horizontal baffles. It can be concluded that the smaller tank size leads to the less impact of sloshing due to some reasons such as increased tank size that tends to increase the highest natural sloshing period and the internal structures dampen the fluid motions [4].

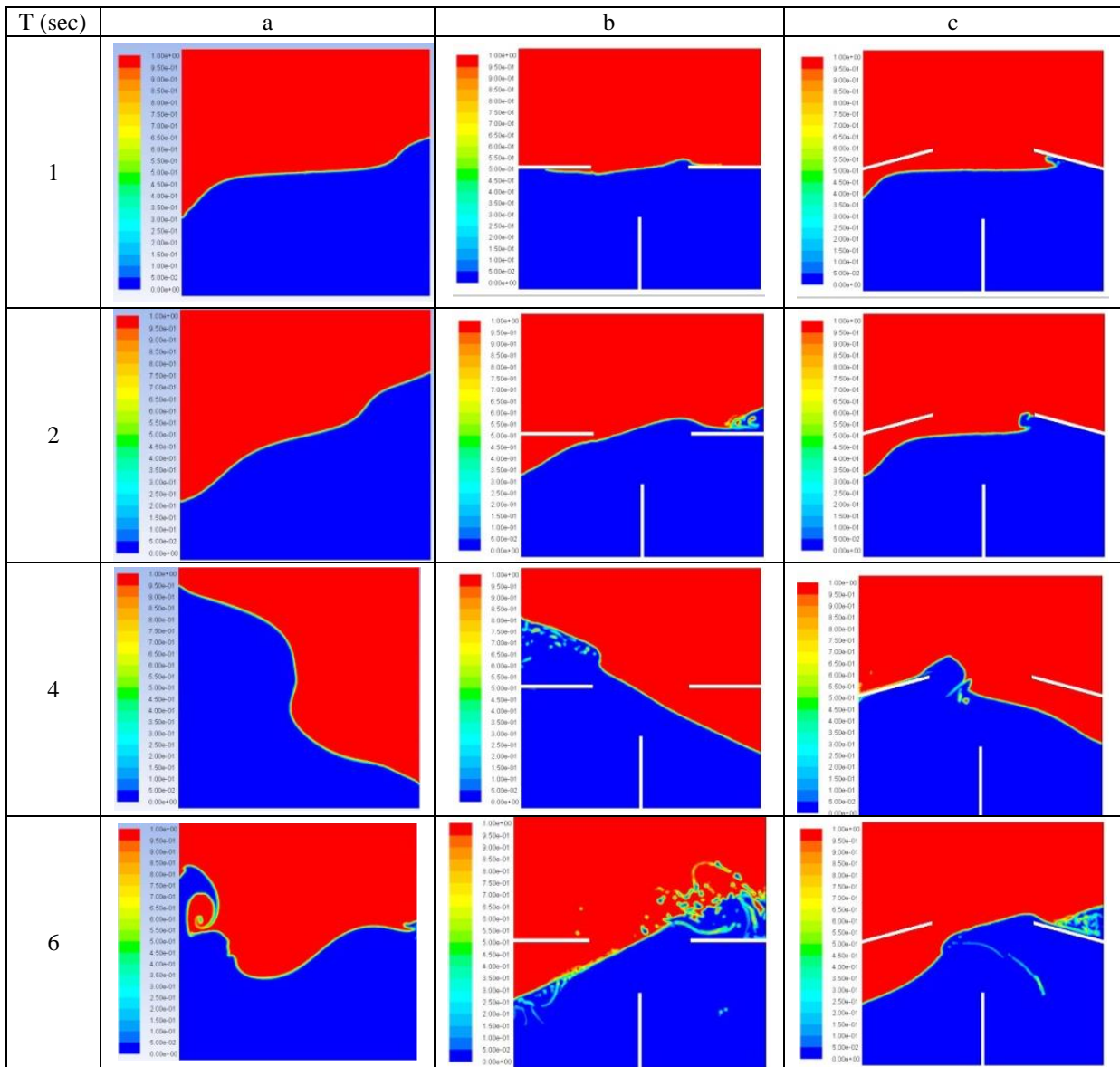


Fig. 4. Sloshing motion at different times for a) Type-1 tank, b) Type-2 tank and c) Type-3 type

At the beginning, type-1 tank seems the worst while Type-2 is the best because the movement of the water towards the left and right side walls can be prevented. Type-3 is better than Type-1, however, worse than Type-2. On the other hand, when time goes by Type-3 tank prevents the sloshing and reduces its effects on side walls. In addition to this, Type-2 prevents violent and overturning and breaking waves that reduce the effects of impact of water on the walls. Since the goal of the sloshing is to study the sloshing pattern and improve the tank design to reduce noise levels, stresses on the structure and optimize the baffle arrangements it can be concluded that Type-3 is the most appropriate among others.

Fig.5 presents the turbulence kinetic energy (TKE) field. It is obvious that baffles distribute the TKE towards

the center in a small region. The similar conclusion was drawn by Akyildiz and Celebi [12] and Celebi and Akyildiz [17] who investigated the effects of a vertical baffle in a rectangular tank. At the first seconds the TKE intensity is higher than the subsequent time and baffles concentrate the TKE towards the center of the tanks.

From the velocity vectors the direction of the movement of the fluid is clearly seen (Fig.6). During its excitation the water affects the air and enforces it to move in the direction of itself. At the beginning, a circulation region is generated and then it is distorted and its movement becomes irregular in Type-1 tank. A similar behavior of the fluid is seen in the other types of tanks but unlike the former one, four recirculation regions are formed below and over the horizontal baffles.

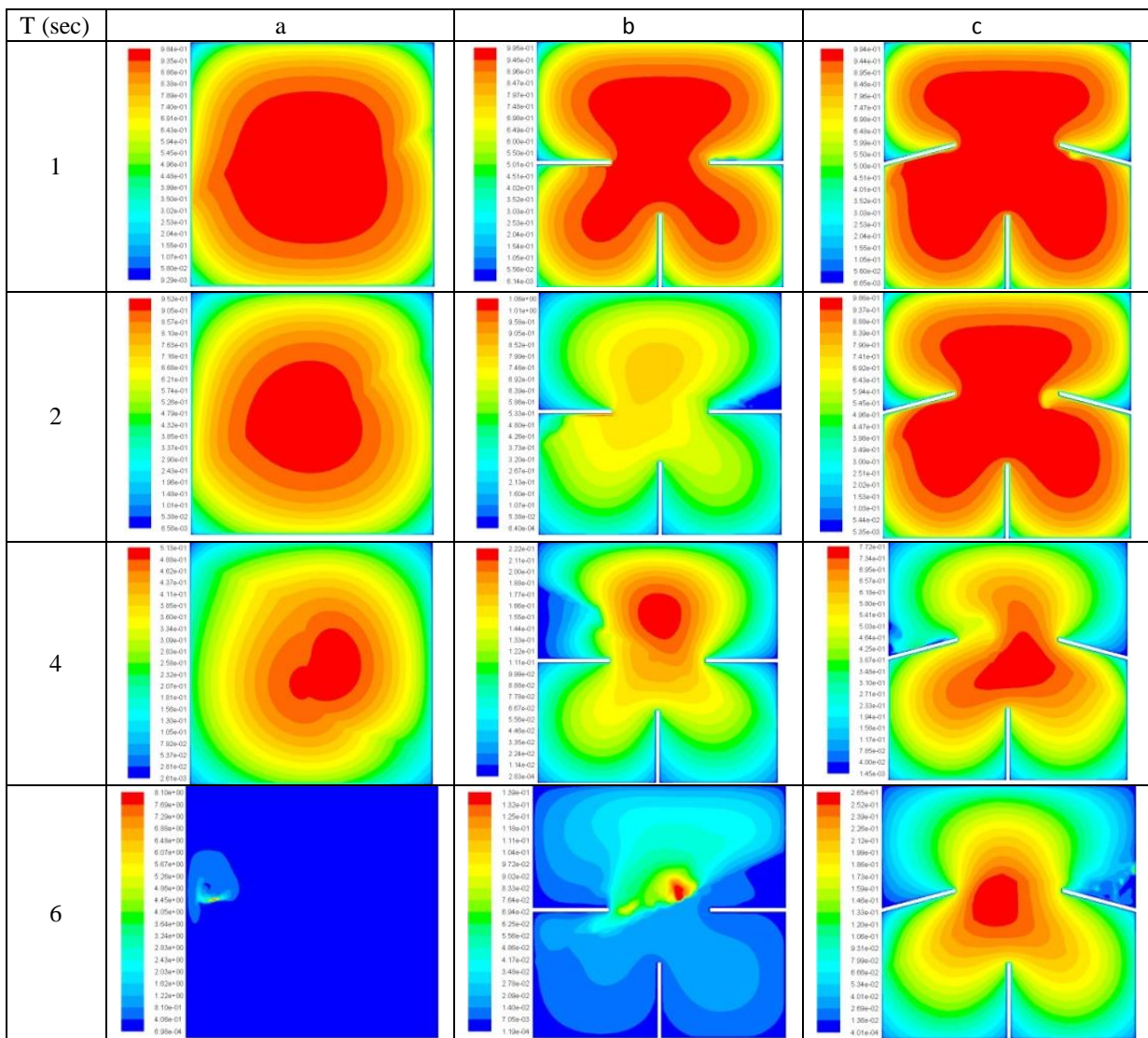


Fig. 5. Turbulence kinetic energy variations in a) Type-1 tank, b) Type-2 tank and c) Type-3 tank

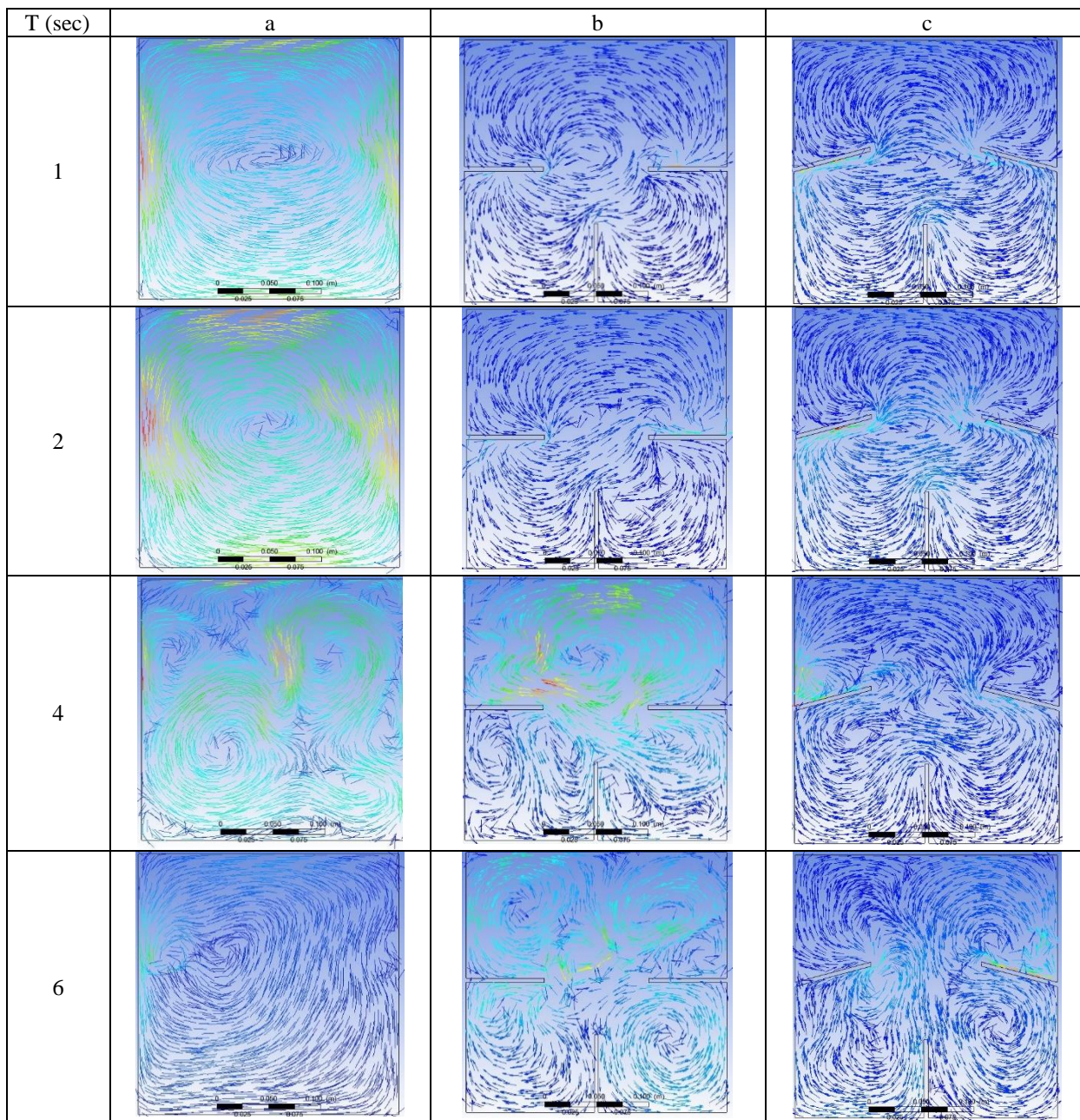


Fig. 6. Velocity vectors in a) Type-1, b) Type-2, c) Type-3

5. Conclusion

In the present CFD study, three types of tanks are analyzed under the same conditions. The computational results show that upward-angled baffles reduce the liquid sloshing amplitude than the other types. Type-2 and Type-3 is the configurations that the tanks is divided into mainly three regions; top, left and right regions. Although these type of configurations reduce the effects of sloshing it was concluded that most ship owners may not want to use such internal structures in cargo tanks because they may not enable the workers to easier cleaning. However, baffles prevents the rise of fluid towards the walls of the tank and therefore, reduces the sloshing effects that increases the life of the structural elements.

References

- [1] Bureau Veritas, Guidance Note, Design Sloshing Loads for LNG Membrane Tanks, May 2011.
- [2] Koli, G.C., Kulkarni, V.V., Simulation of Fluid Sloshing in a Tank, Proceeding of the World Congress on Engineering, WCE 2010, June 30-July 2, 2010.
- [3] Wu, C., Chen, B., Transient Response of Sloshing Fluid in a Three Dimensional Tank, Journal of Marine Science and Technology, vol.20, no.1, pp.26-37.
- [4] Faltinsen, O.M., Rognebakke, O.F., Effect of sloshing on ship motions, 16th International Workshop on Water Waves and Floating Bodies, Hiroshima, Japan, 2001.
- [5] Rudman, M., Cleary, P.W., Modeling Sloshing in LNG Tanks, 7th International Conference on CFD in the

- Minerals and Process Industries, CSIRO, Melbourne, Australia, 9-11 December 2009.
- [6] Det Norske Veritas, Classification Notes on Sloshing Analysis of LNG Membrane Tanks, No.30.9, August 2014. Krata, P., Model of Interaction of Water and Tank's Structure in Sloshing Phenomenon, International Journal of Marine Navigation and Safety of Sea Transportation, vol.2, no.4, December 2008.
- [7] Krata, P, Model of Interaction of Water and Tank's Structure in Sloshing Phenomenon, International Journal of Marine Navigation and Safety of Sea Transportation, Vol.2, No.4, 2008.
- [8] Wemmenhove, R., Luppens, R., Veldman, A.E.P., Bunnik, T., Numerical Simulation and Model Experiments of Sloshing in LNG Tanks, International Conference on Computational Methods in Marine Engineering, MARINE 2007, Barcelona, Spain.
- [9] Hou, L., Li, F., Wu, C., A Numerical Study of Liquid Sloshing in a Two-Dimensional Tank under External Excitations, J. Marine Sci. Appl., 11, 305, 310, 2012.
- [10] Shoji, Y., Munakata, H., Sloshing of Cylindrical Tank due to Seismic Acceleration, Abaqus Users Conference, Newport, Rhode Island, May 2008.
- [11] Xue-Lian, Z., Xian-Sheng, L., Yuan-yuan, R., Equivalent Mechanical Model for Lateral Liquid Sloshing in Partially Filled Tank Vehicles, Mathematical Problems in Engineering, vol.2012, article ID 162825, 2012.
- [12] Akyildiz, H., Celebi, M.S., Numerical Computation of Hydrodynamic Loads on Walls of a Rigid Tank due to Large Amplitude Liquid Sloshing, Turkish J. of Eng. Sci., 26, 429-445, 2002a.
- [13] Javanshir, A., Elahi, R., Passandideh-Fard, M., Numerical Simulation of Liquid Sloshing with Baffles in the Fuel Container, the 12th Iranian Aerospace Society Conference, Amir Kabir University of Technology, 2013.
- [14] Nema, P.K., Computational Study of Sloshing Behavior in 3-D Rectangular Tank with and without Baffle under Seismic Excitation, MSc Thesis, Department of Mechanical Engineering, National Institute of Technology, Rourkela, India, 2014.
- [15] White, F.M., Fluid Mechanics, 5th Edition, McGraw-Hill.
- [16] Kim, Y., Experimental and Numerical Analyses of Sloshing Flows, Journal of Engineering Mathematics, vol.58, issue 1-4, pp.191-210, 2007.
- [17] Celebi, M.S., Akyildiz, H., Nonlinear Modelling of Liquid Sloshing in a Moving Rectangular Tank, Ocean Engineering, vol.29, issue 12, pp.1527-1553, 2002b.

A Comparison of Experimental and Estimated Data Analyses of Solar Radiation, in Adiyaman, Turkey

Haci Sogukpinar *‡, Ismail Bozkurt **, Nazif Calis ***

*Department of Energy Systems Engineering, Faculty of Technology, University of Adiyaman, Adiyaman 02040, Turkey

**Department of Mechanical Engineering, Faculty of Engineering, University of Adiyaman, Adiyaman 02040, Turkey

***Department of Management, Faculty of Economics and Administrative Sciences, University of Adiyaman, Adiyaman 02040, Turkey

(hsogukpinar@adiyaman.edu.tr, ibozkurt@adiyaman.edu.tr, ncalis@adiyaman.edu.tr)

‡ Corresponding Author; First Author, Department of Energy Systems Engineering, Faculty of Technology, University of Adiyaman, Adiyaman 02040, Turkey, Tel: +90 416 223 38 00/2840, hsogukpinar@adiyaman.edu.tr

Received: 25.08.2015 Accepted: 17.09.2015

Abstract- The world's main energy source is the sun. Other energy sources are caused directly or indirectly from the sun. Turkey has a rich potential in terms of solar energy and interest in solar power systems is increasing in the rapidly evolving technology. In all of the solar energy studies needs solar radiation data but solar radiation measurements are not possible on each area. Therefore, estimation of the solar radiation by using a variety of methods is emerging importance. In this study, Turkey and Adiyaman solar energy potential is investigated and statistical analysis was performed for Adiyaman. Various parameters were estimated by using actual solar radiation data from the Meteorology and experimental data were compared with theoretical ones. According to the results of the statistical analyzes, Adiyaman data indicate the best fit with the cubic model.

Keywords: Adiyaman sunshine duration, Turkey solar map, Global solar radiation, Angström-Prescott model

1. Introduction

Increasing energy demand, shortage of fossil fuels and environmental concerns gives impetus to the development of renewable and sustainable energy sources such as solar, geothermal and wind power. [1]. Turkey has rich reserves of renewable and sustainable energy. Among the renewable energy resources in Turkey, one of the most significant one is the solar power [2]. Turkey's average annual solar radiation is 1311 kWh/m²-year, and has 2640 hours of sunshine duration. In all studies related with solar energy systems are needed to solar radiation data and solar radiation measurement is not possible in everywhere. Therefore, the solar radiation must be predicted by using a variety of methods. Complete and accurate solar radiation data for a particular region is inevitable. For a place the measured values are not available, various models have been improved to estimate solar radiation. In the literature, there are various experimental methods used to predict the global solar radiation [3]. Yorukoglu and Celik [4] used five different

models to estimate global solar radiation by using sunshine duration. Daut et. al. [5] suggested a new method which is combination of linear regression and Hargreaves method to estimate the solar radiation. Prieto et. al. [6] improved the correlation between monthly average radiation data and air temperature corresponding to the same temporal sequence of measurements. Papakostas et. al. [7] studied to forecast ambient dry bulb temperature bin-data, based on only the monthly mean temperatures and the solar clearness indicator. Almorox et. al. [8] proposed a new experimental model to intercourse the global solar radiation (H) with its theoretical possible maximum value (H_o), through daily maximum and minimum air temperature.

In this study, statistical analysis was conducted using 6-year Adiyaman solar data. Models such as the linear, quadratic, cubic, logarithmic and exponential are used for this purpose. According to the statistical results, Adiyaman data showed the best fit with cubic model. However, quadratic, logarithmic and exponential model shows best fit after cubic model. By using estimated parameters, solar

radiation values can be estimated for other region. According to the analysis Adiyaman is one of the leading cities in terms of radiation and sunshine duration.

2. Solar energy potential

Turkey is a very rich country in terms of solar energy. Turkey's solar map is given in Figure 1. According to Figure 1, especially in the southern and south eastern part of Turkey is very rich in solar radiation. The highest solar radiation potential from 1800 to 2000 kWh/m²-year comprises in the south-east and south-western areas.



Fig. 1. Turkey’s solar map [9]

Adiyaman, as located west of the Southeastern Anatolia, is one of the provinces where solar energy potential is highest in Turkey. Adiyaman solar map is given in Figure 2. According to Figure 2 solar energy potential ranged from 1600 to 1750 kWh /m²-year in Adiyaman.

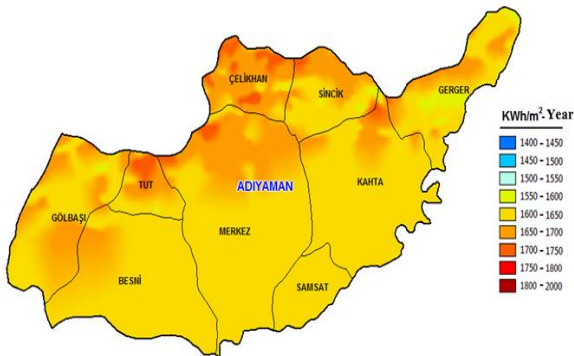


Fig. 2. Adiyaman’s solar map [9]

Measurements of the solar radiation and sunshine duration were made in central part of Adiyaman (38° 17' E, 37° 46' N) in between 2005 to 2010 by Meteorological Office [10]. Figure 3 shows Adiyaman solar radiation measurements for six year. As shown in Figure 3, monthly average solar radiation shows little change according to the measurement years. However, general distribution is carried out in a similar manner. Considering the annual average for six year, lowest average with the value of 1.90 kWh/m²-day takes placed in December and highest value is in June with 7.00 kWh/m²-day.

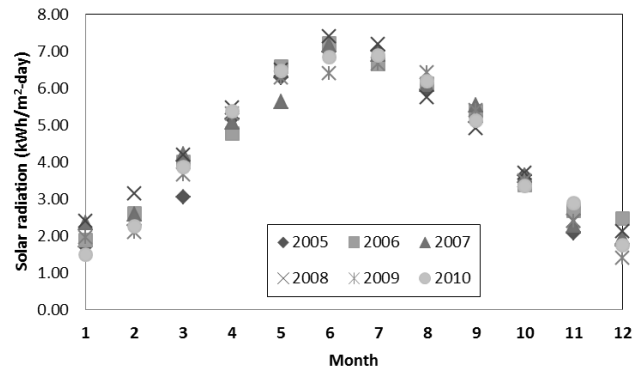


Fig. 3. Adiyaman’s solar radiation data from 2005 to 2010

Adiyaman sunshine duration in between 2005 to 2010 was shown in Figure 4. As shown in figure, maximum daily average sunshine duration by month was achieved in July with value of 12.28 h/day and lowest in January with 3.70 h/day. Adiyaman is one of the province in Turkey with having the highest average sunshine duration (10 h) over 5 months of the year (May-Sep.). Meteorological data seems to be similar by measurement years. Therefore, meteorology has stopped taking new measurements for Adiyaman after 2010.

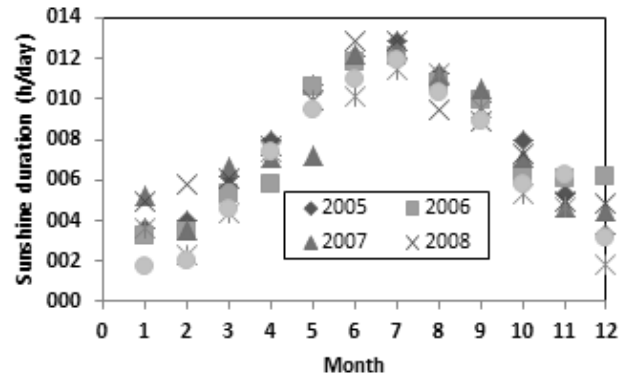


Fig. 4. Adiyaman sunshine duration from 2005 to 2010

3. A Case Study

Statistical analyzes were performed using solar radiation and sunshine duration data that was conducted from 2005 to 2010 in Adiyaman (38° E46' 17' N). Anström-Prescott equation is used to analyze the data. Daily extraterrestrial radiation on horizontal surface for Adiyaman is calculated using equation (1) [11].

$$H_0 = \frac{24 \times 3600}{\pi} G_{sc} \cdot k (\cos \phi \cos \delta \sin \omega_s + \frac{\pi \omega_s}{180} \sin \phi \sin \delta) \quad (1)$$

Here, G_{sc} solar coefficient (1367 W/m²), k is eccentricity correction constant and calculated by equation (2) [11].

$$k = 1 + 0,033 (\cos \frac{360n}{365}) \quad (2)$$

Here, n is representing the number of days starting from the first day of January. δ is declination angle and calculated with Cooper equation (3) [11]:

$$\delta = 23.45 \left(360 \frac{284+n}{365} \right) \tag{3}$$

ω_s is sunset hour angle and expressed equation (4) [11]:

$$\omega_s = \cos^{-1}(-\tan\phi \tan\delta) \tag{4}$$

Regional day length (S_0) is expressed with equation (5) [11]

$$S_0 = \frac{2\omega_s}{15} \tag{5}$$

Statistical analyzes were performed by using linear, quadratic, cubic, logarithmic and exponential models. The models used in the analysis are given in Table 1 and comparison parameters used in the regression analysis are given in Table 2.

Table 1. The regression model used in data analysis

Linear model	$\frac{H}{H_0} = a + b \frac{S}{S_0}$
Quadratic Model	$\frac{H}{H_0} = a + b \frac{S}{S_0} + c \left(\frac{S}{S_0} \right)^2$
Cubic Model	$\frac{H}{H_0} = a + b \frac{S}{S_0} + c \left(\frac{S}{S_0} \right)^2 + d \left(\frac{S}{S_0} \right)^3$
Logarithmic model	$\frac{H}{H_0} = a + b \log \frac{S}{S_0}$
Exponential model	$\frac{H}{H_0} = ae^{b \left(\frac{S}{S_0} \right)}$

Table 2. Comparison parameters used in the regression analysis

$R_1^2 = 1 - \frac{\sum_{i=1}^n \left(\frac{H_{i,m} - H_{i,c}}{H_{i,o}} - \frac{H_{i,c}}{H_{i,o}} \right)^2}{\sum_{i=1}^n \left(\frac{H_{i,m} - \bar{H}_m}{H_{i,o}} - \frac{\bar{H}_m}{H_{i,o}} \right)^2}$	$R_2^2 = 1 - \frac{\sum_{i=1}^n (H_{i,m} - H_{i,c})^2}{\sum_{i=1}^n (H_{i,m} - \bar{H}_m)^2}$
$RMSE_1 = \sqrt{\frac{1}{n} \left(\frac{H_{i,m}}{H_{i,o}} - \frac{H_{i,c}}{H_{i,o}} \right)^2}$	$RMSE_2 = \sqrt{\frac{1}{n} (H_{i,m} - H_{i,c})^2}$
$MBE_1 = \frac{1}{n} \sum_{i=1}^n \left(\frac{H_{i,m}}{H_{i,o}} - \frac{H_{i,c}}{H_{i,o}} \right)$	$MBE_2 = \frac{1}{n} \sum_{i=1}^n (H_{i,m} - H_{i,c})$
$MABE_1 = \frac{1}{n} \sum_{i=1}^n \left(\left \frac{H_{i,m}}{H_{i,o}} - \frac{H_{i,c}}{H_{i,o}} \right \right)$	$MABE_2 = \frac{1}{n} \sum_{i=1}^n (H_{i,m} - H_{i,c})$
$MPE_1 = \frac{1}{n} \sum_{i=1}^n \left(\frac{H_{i,m} - H_{i,c}}{H_{i,m}} \right) 100$	$MPE_2 = MPE_1$
$MAPE_1 = \frac{1}{n} \sum_{i=1}^n \left(\left \frac{H_{i,m} - H_{i,c}}{H_{i,m}} \right \right) 100$	$MAPE_2 = MAPE_1$

4. Results and Discussion

Solar energy systems applications always need solar data. These meteorological data are measured experimentally in several centers. But it is not possible to measure in everywhere. Instead, regression analysis is performed to

create a model to estimate solar data for other region. Regression analysis is a statistical technique that is characterized by a mathematical model in order to estimate the variables in the relationship. Correlation coefficient is calculated to determine whether the reliability of the results obtained in this assay. In this study, experimental measurements were conducted for solar radiation in between 2005-2010 was analyzed statistically by using regression analysis for different models. Statistical analysis results are shown in Table 3. Table 3 reveals that the cubic model showed the best fit to the data for Adiyaman. However, quadratic, exponential and logarithmic model showed the best fit after the cubic model. There is a little difference between the cubic model with other models. This type of modeling with the assistance of the parameters estimated from data for certain region helps to predict solar values of other nearby regions. Solar maps covering the whole country is obtained as a result of modeling by using measurements in certain regions. The same method is applied to determine the country's wind the map. According to the wind measurements made at certain places, other parts of the region are estimated using various models and wind maps prepared.

Daily extraterrestrial radiation on horizontal surface for Adiyaman was calculated using equation (1). Solar radiation measurements data from 2005 to 2010 reaching on horizontal surface were taken from meteorology of Adiyaman. Taking the average of the data received, values of solar radiation reaching on the horizontal surface was found. Figure 5 shows the values of extraterrestrial and terrestrial solar radiation reaching on horizontal surface as monthly average for Adiyaman. As seen in Figure 5, the highest extraterrestrial solar radiation was calculated as 11.58 kWh/m²-day for June, and the lowest one was 4.16 kWh/m²-day in December. Considering measurements of solar radiation reaching on horizontal surface, the highest solar radiation with 7.00 kWh/m²-day was measured in June, the lowest one is 1.90 kWh/m²-day in December. Cloudiness index is defined as the ratio of the monthly average solar radiation to extraterrestrial average solar radiation on the horizontal surface. According to the data given in Figure 5 cloudiness index took placed with the value of 0.42 in February, highest with 0.61 in July. Cloudiness index is quite important in solar energy applications. When calculating the solar energy incident on horizontal surface, index of cloudiness should be considered.

Day length for Adiyaman was calculated using equation (5). Sunshine duration was obtained by observations made by meteorology. Figure 6 shows the day length and sunshine duration for Adiyaman. As shown in Figure 6 maximum day length took placed in June with the value of 14.59 h, and minimum took place in December with 9.40 h. With respect to sunshine duration, maximum day length took placed in July with 12.28 h, and minimum in February with 3.51 h. Although the sunshine duration showed similar changes yearly but according to the cloudiness index seasonal variations may occur. For example, in February sunshine duration is the shortest while the day length is not.

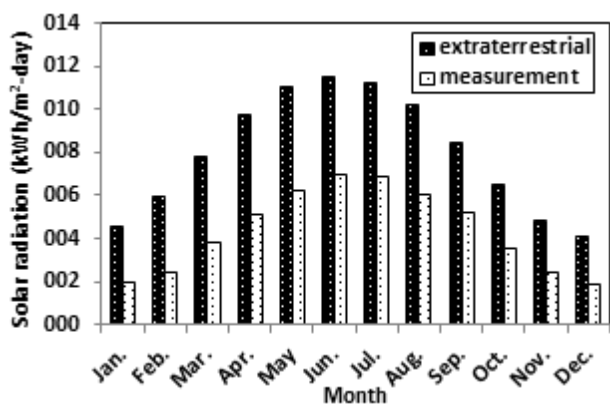


Fig. 5. Terrestrial and extraterrestrial radiation on horizontal surface for Adiyaman

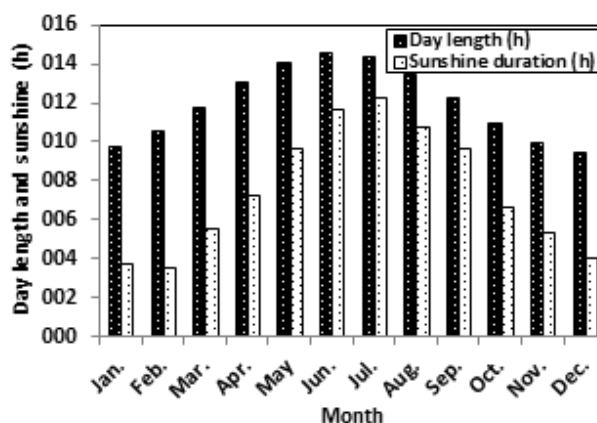


Fig. 6. Day length and sunshine duration for Adiyaman

Table 3. Regression results and statistical parameters for a variety of models for Adiyaman.

	R_1^2	R_2^2	RMSE ₁	RMSE ₂	MBE ₁	MBE ₂	MABE ₁	MABE ₂	MPE ₁	MAPE ₁
Linear	0.772	0.972	0.0445	1.1641	0.0003	0.0318	0.0336	0.8941	-1.06	7.24
Quadratic	0.789	0.976	0.0429	1.0772	0.0001	0.0454	0.0311	0.8087	-0.95	6.73
Cubic	0.793	0.977	0.0424	1.0725	0.0004	0.0523	0.0309	0.8035	-0.88	6.68
Logarithmic	0.746	0.974	0.0470	1.1234	0.0001	0.0926	0.0333	0.8465	-1.00	7.42
Exponential	0.740	0.965	0.0475	1.3093	0.0032	0.0682	0.0371	1.0202	-0.41	7.80

5. Conclusion

Energy is the foremost of today's most important issues. Countries that produce their own energy are being more powerful economically but foreign energy-dependent countries are experiencing serious difficulties. Effects of global warming, which manifests itself in the last 50 years has led the country to renewable energy sources. In this study, statistical analysis was carried out using solar radiation data from 2005 to 2010 for Adiyaman. Linear, quadratic, cubic, logarithmic and exponential models are used in statistical analysis. In used models cubic model showed the best fit for these data. However, Quadratic, exponential, logarithmic, and linear models showed the best correlation after the cubic model respectively. Using this model, radiation values for other regions can be approximated. Thus, it is not necessary to measure the solar radiation in everywhere.

Acknowledgement

The authors are thankful to Turkish State Meteorological Service for wind speed data.

Nomenclature

- $a-d$ empirical constants
- G_{sc} solar constant ($G_{sc} = 1367 \text{ W/m}^2$)
- H daily global solar radiation on horizontal surface (MJ/m^2)
- H_o daily extraterrestrial radiation on horizontal surface (MJ/m^2)
- n number of day of year starting from first of January
- k eccentricity correction factor

- R^2 coefficient of determination
- S sunshine duration (h)
- S_o day length (h)

Greek letters

- ω_s sunset hour angle (degree)
- δ solar declination (degree)
- ϕ latitude of site (degree)
- σ standard deviation

Acronyms

- MAE mean absolute error
- MABE mean absolute bias error
- MAPE mean absolute percentage error
- MBE mean bias error
- MPE mean percentage error
- NSE Nash–Sutcliffe equation
- RMSE root mean square error
- SEE standard error of estimate

References

- [1] I. Dincer, M.A. Rosen, "Thermal energy storage: systems and applications", New York: John Wiley and Sons, 2003.
- [2] M. Balat, "The use of renewable energy sources for energy in Turkey and potential trends", Energy Explor Exploit, 22: 241–57, 2004.
- [3] J. Almorox, M. Bocco, "Enrique Willington, Estimation of daily global solar radiation from measured temperatures at Cañada de Luque, Córdoba, Argentina", Renewable Energy 60: 382-387, 2013.

- [4] M. Yorukoglu, A.N. Celik, "A critical review on the estimation of daily global solar radiation from sunshine duration", *Energy Conversion and Management* 47: 2441–2450, 2006.
- [5] I. Daut, M. Irwanto, Y.M. Irwan, N. Gomesh, N.S. Ahmad, "Combination of Hargreaves method and linear regression as a new method to estimate solar radiation in Perlis, Northern Malaysia", *Solar Energy* 85: 2871–2880, 2011.
- [6] J.I. Prieto, J.C. Martinez-Garcia, D. Garcia, "Correlation between global solar irradiation and air temperature in Asturias, Spain", *Solar Energy* 83: 1076–1085, 2009.
- [7] K. Papakostas, A. Bentoulis, V. Bakas, N. Kyriakis, "Estimation of ambient temperature bin data from monthly average temperatures and solar clearness index. Validation of the methodology in two Greek cities", *Renewable Energy* 32: 991–1005, 2007.
- [8] J. Almorox, "Estimating global solar radiation from common meteorological data in Aranjuez, Spain", *Turk J Phys* 35: 53 – 64, 2011.
- [9] General Directorate of Renewable Energy (EIE), "Solar map", Available at: <[http:// www.eie.gov.tr](http://www.eie.gov.tr), 2015.
- [10] Meteorology Regional Offices, , Turkish State Meteorological Service, Ankara, Turkey. Available at: <[http:// www.mgm.gov.tr](http://www.mgm.gov.tr), 2015.
- [11] J.A. Duffie, W.A. Beckman, "Solar Engineering of Thermal Processes", second ed. John Wiley & Sons Inc., New York, 1991.

Modelling of Instant Solar Radiation Using Average Instant Temperature of Ogbomoso, South Western, Nigeria

Oluwaseun Adedokun*, Aishat Abidemi Abass, Yekinni Kolawole Sanusi

Department of Pure and Applied Physics, Ladoké Akintola University of Technology, P.M.B. 4000, Ogbomoso, Nigeria

(oadedokun@lautech.edu.ng, abass.aishat36@yahoo.com, yksanusi@lautech.edu.ng)

*Corresponding Author: Oluwaseun Adedokun, Department of Pure and Applied Physics, Ladoké Akintola University of Technology, P.M.B. 4000, Ogbomoso, Tel: +234 7031195750, oadedokun@lautech.edu.ng

Abstract - The paper is aimed at proffering an alternative means to the meteorological measuring stations by generating models for average instant solar radiation as a function of instant average temperature at places where measurement are not available. The data were processed using Microsoft excel software programming and regression analysis to generate a set of models for both morning and afternoon sessions of instant solar radiation of Ogbomoso as a function of temperature. In order to validate these models, statistical indicators like RMSE, MBE and MPE were used. The value of RMSE, MBE and MPE statistical indicators for morning and afternoon set of data were calculated to be 0.001219, -0.0000002, 0.0059% and 0.00033769, -0.00171225, -4.82%, respectively. From the t-test statics, percentage error between the measured and calculated values of instant average temperature, it is revealed that the set of models in this work can adequately be used in place of the data from the measuring stations since there is complementary relationship between the measured and the calculated instant solar radiation of Ogbomoso. And this modelling result could be used in the estimation of instant solar radiation at locations where measurements are not available to design high performance solar radiation related devices.

Keywords: Instant solar radiation, average instant temperature, modelling, statistical indicators, Nigeria

1. Introduction

Energy is the motive force behind the continual technological improvement of any nation and Nigeria is blessed with reasonably high quantities of various energy resources [1]. The time needed to develop a new source of energy, such as solar energy, can be provided through the conservation of energy resources. Solar radiation passing through the atmosphere to the ground surface is known to be depleted through scattering, reflection and absorption by the atmospheric constituents like air molecules, aerosols, water vapour, ozone and the clouds. In any conversion of solar energy, the understanding of global solar radiation is essential in achieving a quality design and the expectation of the system performance. Practically, solar radiation data is the most important parameter in the design and evaluation of solar energy devices. An accurate knowledge of solar radiation distribution at a particular geographical location is of vital importance for surveys in agronomy, hydrology, eulogy and sizing of the photovoltaic or thermal solar systems and estimates of their performance. To collect the solar radiation data, a system of solar maintaining station fitted out with pyranometer and data gain system are generally founded in the

desired locations which is used by researchers to extrapolate values for places of similar climatological and geographical characteristics at which solar records are unavailable. A Few numbers of such stations are in Nigeria and insufficient to present reports of solar radiation on desired locations especially in developing countries. This is due to their inability to afford the measuring equipment and lack of maintenance and calibration of the equipment. In other to solve this problem an approach is used here to model an equation to estimate instant solar radiation as a function of instant average temperature to be used in places where measurement are not available. Instant temperature is easy to measure using digital thermometer which is affordable. Another approach is comparing the global solar radiation to climatological data at the location where the data is collated. The first empirical correlation using sunshine hours for estimation of solar radiation was proposed by Angstrom [2]. This model was later modified by Prescott and Page [2- 4] in which the model is given as:

$$\frac{H}{H_o} = a + b \frac{S}{S_o} \quad (1)$$

Where H is the monthly average daily global radiation on horizontal surface, H_0 is the monthly average daily extra-terrestrial radiation, S is the length of the day, S_0 is the maximum possible sunshine duration, and a and b are constants. Since this development, there have been other models such as Rietveld, Bahel, Glover, Hay and Grag models [5]. Akpabio *et al.* [6] developed the quadratic form of Angstrom-Prescott model and used it to estimate the global solar radiation at Onne, Nigeria (latitude $4^{\circ} 46' N$, Longitude $7^{\circ} 10' E$). Multi-linear polynomial form of the Angstrom-Prescott model was employed by Agbo *et al.* [7] to estimate global solar radiation at Minna, Nigeria. Various other models employing other meteorological parameters with one or more variables with solar radiation have also been used. The estimation of the solar radiation at Uturu in Nigeria was carried out using an equation relating solar radiation and temperature [8]. Agbo [9] had also estimated 'global' solar radiation at Onitsha using regression analysis and artificial neural network models with the attendant parameters of temperatures and relative humidity. Here in this work, models were formulated using a simple method and statistical indicators such as (RMSE, MPE, MSE, r and r^2), curve tracing, t-test statistics, were used to validate the models estimated.

2. Materials and Methods

The monthly mean daily data for maximum ambient temperature and the solar radiation data for Ogbomosho were collected from the Archives of the Nigerian Meteorological Agency (NIMET), Lagos, Nigeria. The data obtained covered a period of a year for Ogbomoso at Latitude 8.3° and Longitude 4.3° . The data obtained were processed to hourly average in preparation for the correlation between instant solar radiation and instant average temperature.

Some given temperature comprises of two values, so we cannot get the solar radiation as a single valued function of temperature for these data. In other to obtain radiation as the function of temperature, we use Excel software program to break down the data at the turning point and get relation of instant solar radiation with instant temperature for morning hours and evening hours separately. Percentage errors will be estimated between the values obtained from the Metrological centre and the values predicted by the developed equation.

2.1. The comparison methods

In this study, evaluation of the accuracy of estimated data from the above described models is done using the following statistical tests, MBE, RMSE, mean percentage error (MPE) and coefficient of correlation (r). Correlation between predicted and measured values is tested using Curve tracing process.

2.2. The root mean square error, mean bias error and mean percentage error

The Root Mean Square Error (RMSE) (also called the root mean square deviation, RMSD) is a frequently used measure of the difference between values predicted by a model and the values actually observed from the environment that is being

modelled. These individual differences are also called residuals, and the RMSE serves to aggregate them into a single measure of predictive power. The accuracy of the estimate depends on the lower value of RMSE. However, an increase in RMSE can be caused by a few large errors in the sum. Obviously, every single test may not be a suitable indicator of a pyranometer's performance. It is possible to have a large RMSE value and simultaneously a small MBE (a large scatter about the line of perfect measurement) or possibly vice-versa i.e a small RMSE and large MBE (consistently small over- or under measurement). Although these statistical indicators generally gives a reliable procedure to compare models, but do not accurately indicate whether a model's measures are statistically significant, that is, not significantly different from their predicted counterparts. In this article, t-statistic was used as an additional statistical indicator. This statistical indicator enables models to simultaneously compare and indicates whether or not a model's measures are statistically valid at a particular reliable level [10]. It was seen that the t-statistic used in addition to the RMSE and MBE gave more reliable and explanatory results [11].

$$RMSE = \left\{ \sum_{i=1}^n \left(\frac{K_{TP} - K_{TM}}{n} \right)^2 \right\}^{1/2} \quad (2)$$

A positive value of mean bias error (MBE) shows an over-estimate while a negative value an under-estimate by the model and the lower the value for a particular model, the better the performance. This test gives information on the long-term performance

$$MBE = \frac{\left\{ \sum_{i=1}^n (K_{TP} - K_{TM}) \right\}}{n} \quad (3)$$

The mean percentage error (MPE) gives long term performance of the examined regression equations, a positive MPE values provides the averages amount of overestimation in the calculated values, while the negatives value gives underestimation. A low value of MPE is desirable [12].

$$MPE = \left\{ \sum_{i=1}^n \left(\frac{K_{TP} - K_{TM}}{K_{TM}} \right) \right\} \times 100 \quad (4)$$

Where K_{TP} is the predicted value K_{TM} is the measured values and n is the total number of observations.

The t-Statistics Test

In one of the tests for mean values as defined by a student [13], the random variable t with n-1 degrees of freedom may be written as follows:

$$t = \sqrt{\left[\frac{(n-1)(MBE)^2}{(RMSE)^2 - (MBE)^2} \right]} \quad (5)$$

The smaller the value of t, the better is the performance. To determine whether a model's estimates are statistically significant, one simply has to determine, from standard statistical tables, the critical t value, i.e. $t_{\alpha/2}$ at α level of significance and (n-1) degrees of freedom. For the model's estimates to be judged statistically significant at the $(1-\alpha)$ confidence level, the calculated t value must be less than the critical value.

3. Results and Discussion

Figure 1 shows a plot of instant solar radiation and instant average temperature for the year 2012. It is obvious that extraction of data here may be difficult. Therefore, in order to simplify the process, the data were grouped as mentioned in previous section. From Table 1, there are two values for some given temperature. So it is difficult to get solar radiation as a single valued function of temperature for these data. In order to get the radiation as the function of temperature, we then break the data at the turning point and get relation of instant solar radiation with instant temperature for morning hours and evening hours separately by using Microsoft Excel.

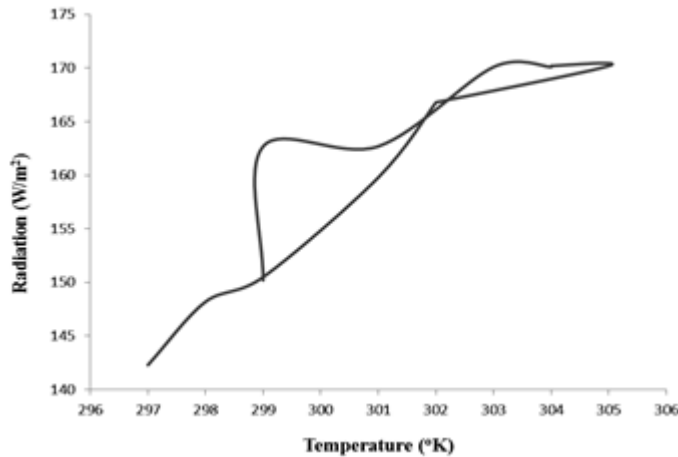


Fig. 1. Instant solar radiation against instant average temperature for the year 2012

Table 1. Instant average temperature and instant solar radiation of Ogbomosho from January 2012 to December 2012

Time (hr)	Instant Solar Radiation (Wm ⁻²)	Instant Temperature (°C)	Instant Temperature (°K)
7:00 am	142.30	24	297
8:00 am	148.20	25	298
9:00 am	150.50	26	299
10:00am	159.80	28	301
11:00 am	166.80	29	302
12:00 pm	166.80	30	303
1:00 pm	170.20	32	305
2:00 pm	170.20	31	304
3:00 pm	170.10	31	304
4:00 pm	170.10	30	303
5:00 pm	162.70	28	301
6:00 pm	162.70	26	299
7:00 pm	150.20	26	299

The relation between the instant solar radiation and instant temperature is to be developed for morning data where 7.00 AM to 11.00AM were taken. And the relation between the instant solar radiation and instant temperature is to be

developed for afternoon data where 12.00 PM to 7.00PM were taken. The data were shown as in the given Table 2 and 3, respectively.

Table 2. Showing reports for morning hours on an instant solar radiation and instant average temperature

Time (hr)	Instant Solar Radiation (Wm ⁻²)	Instant Temperature (°C)	Instant Temperature (°K)
7:00 am	142.30	24	297
8:00 am	148.20	25	298
9:00 am	150.50	26	299
10:00am	159.80	28	301
11:00 am	166.80	29	302

Table 3. Showing reports for afternoon hours on an instant solar radiation and instant average temperature

Time (hr)	Instant Solar Radiation (Wm ⁻²)	Instant Temperature (°C)	Instant Temperature (°K)
12:00 pm	166.80	30	303
1:00 pm	170.20	32	305
2:00 pm	170.20	31	304
3:00 pm	170.10	31	304
4:00 pm	170.10	30	303
5:00 pm	162.70	28	301
6:00 pm	162.70	26	299
7:00 pm	150.10	26	299

The estimated equation from the graph in Figure 2 is obtained using Microsoft excel software as expressed in Equation 6, where the solar radiation (W/m²) is plotted against the instant average temperature(°K) for the morning section from the hour of 7:00 AM to 11:00 AM. The equation has a dependent variable (solar radiation) and an independent variable (temperature) represented as R and T, respectively.

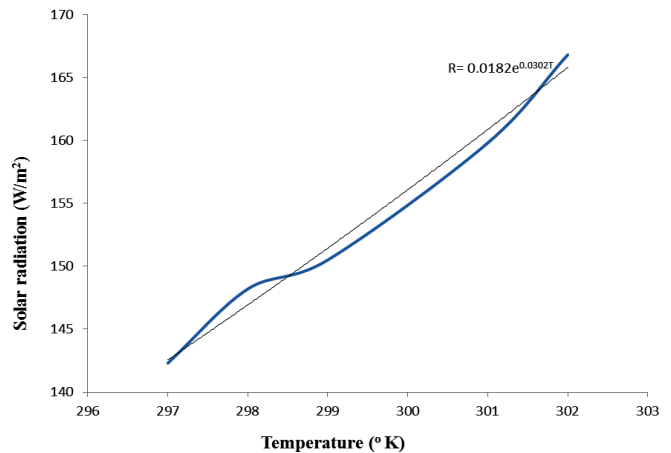


Fig. 2. Showing records for the morning on variation in instant solar radiation and instant temperature

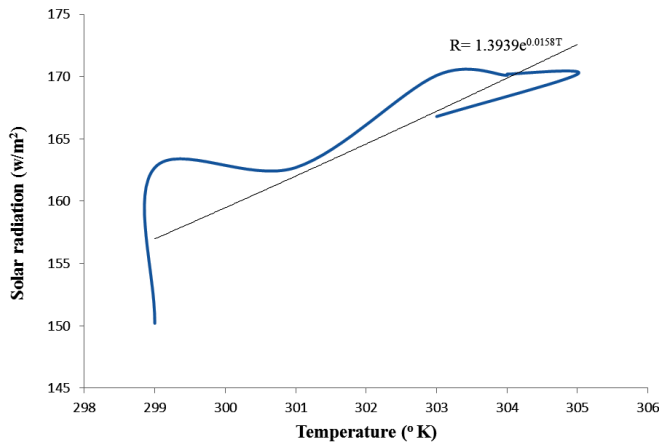


Fig. 3. Showing records for the afternoon on variation in instant solar radiation and instant temperature

$$R = 0.0182e^{0.0302T} \quad (6)$$

The corresponding equation as shown in Equation 7 from the graph in Figure 3 is obtained from the software used given as

$$R = 1.3939e^{0.0158T} \quad (7)$$

Table 4 and 5 provide the value of W_{meas} measured, W_{cal} calculated and the percentage error from the estimated equations for morning and afternoon hours. This is to test for the validity of both morning and afternoon models obtained. As observed from Table 4 and 5, we have a very minimal percentage error and the equation obtained may be taken as valid. From Table 4, it was also observed that there is a normal trend of the temperature values and the solar radiation values from 7:00 am to 11:00 am and also no repetition in the values of both the temperature and the solar radiation measured which gives a high validity of the model estimated from Figure 2.

The graphs in Figure 4 and Figure 5 show the degree of correlation between the measured values gotten from the meteorological centre and the predicted values from the regression analysis. And as evident from curve tracing graphs in Figure 4 and Figure 5 for morning and afternoon hours, respectively, proved the correlation between the measured values and the calculated values of the instant average solar radiation and validity of the estimated model.

From Table 6, it was observed that there is no significant difference in the temperature and solar radiation measured for a particular time throughout the year which gives constant values for both the temperature and the solar radiation. The curve tracing graph for afternoon hours shown in Figure 5 give a greater RMSE value and simultaneously a smaller MBE (a large scatter about the line of perfect measurement). The t-test statistics was used to test for the validity of the estimated models at a confidence level of 95% where the $H_0 (\mu_m - \mu_p = 0)$ since our t_{cal} is greater than t_{tab} for both morning and afternoon hours. It is observed in the curve tracing graph for afternoon hours that it is scatter which can be caused due to

error in the measurement. Error in measurement of solar radiation values can be arise from early morning dew deposition, directional error, shadowing over the sensor and so caused any errors in the measurement or thermopile sensor not responding to radiation atmosphere. The dome made from one or two layers of ground and polished optical glass or acrylic plastic that shields the thermopile sensor from convection at the period of extremely high temperature because loss of heat due to convection which can reduce the solar radiation measured by the pyranometer and also the desiccants which eliminates air movement and dirt that might affect the measurements. The aim of this work is to propose models for instant solar radiation using instant average temperature of Ogbomosho, in Nigeria and the significance of the models is for the estimation of instant solar radiation at places where measurement are not available to design high performance solar radiation related devices.

Table 4. The morning hours data on percentage error and value of W measured and calculated from the equation

W_{Meas}	W_{Cal}	$W_{meas} - W_{cal}$	Percentage error
2.153205	2.154230	-0.001025	-0.04760
2.170848	2.167248	0.00360	0.16583
2.177536	2.180265	-0.002729	-0.12533
2.203577	2.206300	-0.002723	-0.12357
2.222196	2.219318	0.002878	0.12951

Table 5. The afternoon hours data on percentage error and value of W measured and calculated from the equation

W_{Meas}	W_{Cal}	$W_{meas} - W_{cal}$	Percentage error
2.222196	2.221545	0.000651	0.029295
2.23096	2.235242	-0.004282	-0.191935
2.23096	2.228394	0.002566	0.115018
2.230704	2.228394	0.00231	0.103555
2.230704	2.221545	0.009159	0.410588
2.211388	2.207848	0.00354	0.160080
2.211388	2.194152	0.017236	0.779420
2.17667	2.194152	-0.017482	-0.803153

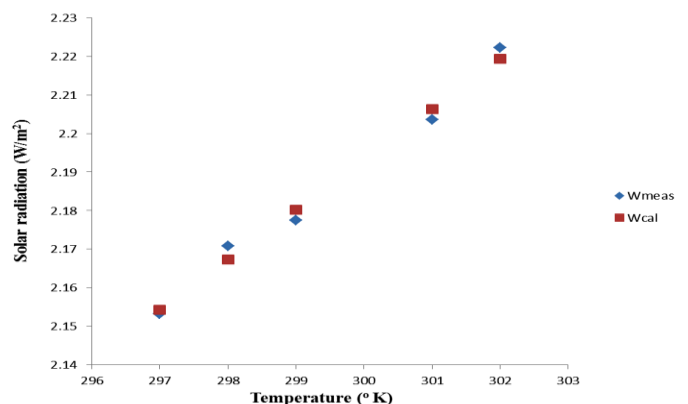


Fig. 4. Curve tracing showing values of W_{cal} and W_m for the morning hours

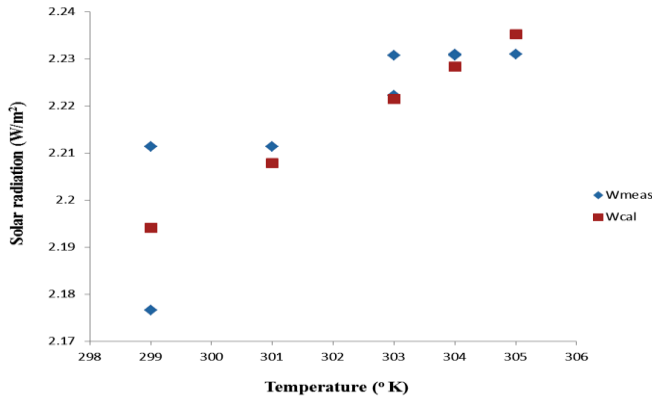


Fig. 5. Curve tracing showing values of W_{cal} and W_m for the afternoon hours

Table 6. The values obtained for statistical indicators used

Statistical Indicators	Morning Hours (7:00am – 11:00 am)	Afternoon Hours (12:00 pm – 7:00 pm)
RMSE	0.001219	0.00033769
MBE	-0.0000002	-0.00171225
MPE	0.0059%	-4.82%

4. Conclusion and Recommendation

The models estimated in this work for the morning and afternoon hours can be used as another method for measuring the values of solar radiation measure using pyranometer for places of similar climatological and geographical characteristics at which solar records are unavailable. This will solve the problem of insufficient number of meteorological stations in Nigeria which is due to their inability to afford the measuring equipment and lack of maintenance and calibration of the equipment. Instant temperature is easy to measure using digital thermometer which is affordable. But this study is only limited to one year data for a particular geographical location. Instant value included in solar radiation and instant temperature values are essential data for design and efficient functioning of various solar thermal and photovoltaic devices. This will also allow user of the data to track information of solar radiation data in Ogbomoso.

For successive development of such types of empirical relations estimating models on the effects of sky clearness index, cloud cover and wind velocity, relative humidity may also be taken into account in developing the relationship for Ogbomoso area. In this study only one year of area data have been used. Validation using sufficient large amount of data for a longer period of years is required for wider application of the method.

Acknowledgement

The authors are grateful to NIMET for providing all the necessary data.

References

- [1] N.N. Gana, K. Ral. Jitendra, Musa Momoh, (2014) “Estimation of Global and Diffuse Solar Radiation for Kebbi, North Western Nigeria”, International Journal of Scientific & Engineering Research, Vol. 5, 1: January 2014, 1654-1661.
- [2] F. Ahmad, I. Ulfat, (2004) “Empirical Models for the correlation of monthly average daily global solar radiation with hours of sunshine on a horizontal surface at Karachi”, Pakistan. Turk. J. Phys. 28:301-307.
- [3] Page, J.K., (1961) “The estimation of monthly mean values of daily total shortwave radiation on vertical and inclined surfaces from sunshine records for latitudes 40°N – 40°S”, In proceedings of UN conference on new sources of energy. pp. 378-390
- [4] A.N. Maghrabi, (2009), “Parameterization of a simple model to estimate monthly global solar radiation bases on meteorological variables and evaluation of existing solar radiation models for Tabouk, Saudi Arabia”, Energy conversion and management. 50: 2754 –2760.
- [5] N.L. Mahdi, N.S. Baharn, F.F. Zaki, (1992) “Assessment of solar radiation models for the Gulf Arabian countries”, Renew. Energy 2(1):65-71.
- [6] L.E. Akpabio, S.O. Udo, S.E. Etuk, (2005) “Modelling Global Solar Radiation for a Tropical Location: Onne, Nigeria”, Turk. J. Phys. 29:63-68.
- [7] G.A. Agbo, A. Baba, T.N. Obiekezie, (2010) “Empirical Models for the correlation of monthly average global solar radiation with sunshine hour at Minna”, Nig. J. B. Res. 1 (1):41-47.
- [8] I.U. Chiemeka, (2008) “Estimation of solar radiation at Uturu, Nigeria”, Inter. J. Phys. Sci. 3 (5):126-130.
- [9] G.A. Agbo, (2012) “Estimation of Global Solar Radiation at Onitsha with Regression analysis and artificial Neural Network Models”, Res. J. Recent. Sci. 1 (6):1-8.
- [10] F.W. Burari, A.S. Sambo, (2001) “Model for the prediction of global solar radiation for Bauchi using Meteorological Data,” Nigeria Journal of Renewable Energy, vol. 91, pp 30 -33.
- [11] A.M. Al-Salihi, M.M. Kadum, A.J. Mohammed, (2010) “Estimation of global solar radiation on horizontal surface using meteorological measurement for different cities in Iraq,” Asian Journal of Scientific Research, vol 3, no 4, pp 240 – 248.
- [12] E.O. Falayi, J.O. Adepitan, A.B. Rabi, (2008) “Empirical models for the correlation of global solar radiation with meteorological data for Iseyin, Nigeria,” International Journal of Physical Sciences, vol. 3, no 9, pp 210 – 216.
- [13] P.R. Bavington, (1969) “Data reduction and error analysis for the physical sciences”, McGraw-Hill; New York.

Guide for Authors

The *International Journal of Engineering Technologies (IJET)* seeks to promote and disseminate knowledge of the various topics of engineering technologies. The journal aims to present to the international community important results of work in the fields of engineering such as imagining, researching, planning, creating, testing, improving, implementing, using and asking. The journal also aims to help researchers, scientists, manufacturers, institutions, world agencies, societies, etc. to keep up with new developments in theory and applications and to provide alternative engineering solutions to current.

The *International Journal of Renewable Energy Research* is a quarterly published journal and operates an online submission and peer review system allowing authors to submit articles online and track their progress via its web interface. The journal aims for a publication speed of **60 days** from submission until final publication.

The coverage of IJET includes the following engineering areas, but not limited to:

All filed of engineering such as;

Chemical engineering

- Biomolecular engineering
- Materials engineering
- Molecular engineering
- Process engineering

Civil engineering

- Environmental engineering
- Geotechnical engineering
- Structural engineering
- Transport engineering
- Water resources engineering

Electrical engineering

- Computer engineering
- Electronic engineering
- Optical engineering
- Power engineering

Mechanical engineering

- Acoustical engineering

- Manufacturing engineering
- Thermal engineering
- Vehicle engineering

Systems (interdisciplinary) engineering

- Aerospace engineering
- Agricultural engineering
- Applied engineering
- Biological engineering
- Building services engineering
- Energy engineering
- Railway engineering
- Industrial engineering
- Mechatronics
- Military engineering
- Nano engineering
- Nuclear engineering
- Petroleum engineering

Types of Articles submitted should be original research papers, not previously published, in one of the following categories,

- Applicational and design studies.
- Technology development,
- Comparative case studies.
- Reviews of special topics.
- Reviews of work in progress and facilities development.
- Survey articles.
- Guest editorials for special issues.

Editorial Board

Editor-in-Chief:

Professor ILHAMI COLAK

Associate Editors:

Dr. Selin ÖZCIRA

Dr. Mehmet YESILYAPRAK

Ethic Responsibilities

The publication of an article in peer-reviewed “*International Journal of Engineering Technologies*” is an essential building block in the development of a coherent and respected network of knowledge. It is a direct reflection of the quality of the work. Peer-reviewed articles support and embody the scientific method. It is therefore important to agree upon standards of expected ethical behavior for all parties involved in the act of publishing: the author, the journal editor, the peer reviewer, the publisher and the society of society-owned or sponsored journals.

All authors are requested to disclose any actual or potential conflict of interest including any financial, personal or other relationships with other people or organizations within three years of beginning the submitted work that could inappropriately influence, or be perceived to influence, their work.

Submission of an article implies that the work described has not been published previously that it is not under consideration for publication elsewhere. The submission should be approved by all authors and tacitly or explicitly by the responsible authorities where the work was carried out, and that, if accepted, it will not be published elsewhere in the same form, in English or in any other language, including electronically without the written consent of the copyright-holder.

Upon acceptance of an article, authors will be asked to complete a “Copyright Form”. Acceptance of the agreement will ensure the widest possible dissemination of information. An e-mail will be sent to the corresponding author confirming receipt of the manuscript together with a “Copyright Form” form or a link to the online version of this agreement.

Author Rights

As a journal author, you retain rights for a large number of author uses, including use by your employing institute or company. These rights are retained and permitted without the need to obtain specific permission from *IJREER*. These include:

- ❖ The right to make copies (print or electronic) of the journal article for your own personal use, including for your own classroom teaching use;
- ❖ The right to make copies and distribute copies (including via e-mail) of the journal article to research colleagues, for personal use by such colleagues for scholarly purposes;
- ❖ The right to post a pre-print version of the journal article on internet web sites including electronic pre-print servers, and to retain indefinitely such version on such servers or sites for scholarly purposes

- ❖ the right to post a revised personal version of the text of the final journal article on your personal or institutional web site or server for scholarly purposes
- ❖ The right to use the journal article or any part thereof in a printed compilation of your works, such as collected writings or lecture notes.

Article Style

Authors must strictly follow the guide for authors, or their articles may be rejected without review. Editors reserve the right to adjust the style to certain standards of uniformity. Follow Title, Authors, Affiliations, Abstract, Keywords, Introduction, Materials and Methods, Theory/Calculation, Conclusions, Acknowledgements, References order when typing articles. The corresponding author should be identified with an asterisk and footnote. Collate acknowledgements in a separate section at the end of the article and do not include them on the title page, as a footnote to the title or otherwise.

Abstract and Keywords:

Enter an abstract of up to 250 words for all articles. This is a concise summary of the whole paper, not just the conclusions, and is understandable without reference to the rest of the paper. It should contain no citation to other published work. Include up to six keywords that describe your paper for indexing purposes.

Abbreviations and Acronyms:

Define abbreviations and acronyms the first time they are used in the text, even if they have been defined in the abstract. Abbreviations such as IEEE, SI, MKS, CGS, sc, dc, and rms do not have to be defined. Do not use abbreviations in the title unless they are unavoidable.

Text Layout for Peer Review:

Use single column layout, double spacing and wide (3 cm) margins on white paper at the peer review stage. Ensure that each new paragraph is clearly indicated. Present tables and figure legends in the text where they are related and cited. Number all pages consecutively; use 12 pt font size and standard fonts; Times New Roman, Helvetica, or Courier is preferred.

Research Papers should not exceed 12 printed pages in two-column publishing format, including figures and tables.

Technical Notes and Letters should not exceed 2,000 words.

Reviews should not exceed 20 printed pages in two-column publishing format, including figures and tables.

Equations:

Number equations consecutively with equation numbers in parentheses flush with the right margin, as in (1). To make equations more compact, you may use the solidus (/), the exp function, or appropriate exponents. Italicize Roman symbols for quantities and variables, but not Greek symbols. Use an dash (–) rather than a hyphen for a minus sign. Use parentheses to avoid ambiguities in denominators. Punctuate equations with commas or periods when they are part of a sentence, as in

$$C = a + b \tag{1}$$

Symbols in your equation should be defined before the equation appears or immediately following. Use “Eq. (1)” or “equation (1),” while citing.

Figures and Tables:

All illustrations must be supplied at the correct resolution:

- * Black and white and colour photos - 300 dpi
- * Graphs, drawings, etc - 800 dpi preferred; 600 dpi minimum
- * Combinations of photos and drawings (black and white and color) - 500 dpi

In addition to using figures in the text, upload each figure as a separate file in either .tiff or .eps format during submission, with the figure number.

Table captions should be written in the same format as figure captions; for example, “Table 1. Appearance styles.”. Tables should be referenced in the text unabbreviated as “Table 1.”

References:

Please ensure that every reference cited in the text is also present in the reference list (and viceversa). Any references cited in the abstract must be given in full. Unpublished results and personal communications are not recommended in the reference list, but may be mentioned in the text. Citation of a reference as “in press” implies that the item has been accepted for publication. Number citations consecutively in square brackets [1]. Punctuation follows the bracket [2]. Refer simply to the reference number, as in [3]. Use “Ref. [3]” or Reference [3]” at the beginning of a sentence: “Reference [3] was ...”. Give all authors’ names; use “et al.” if there are six authors or more. For papers published in translated journals, first give the English citation, then the original foreign-language citation.

Books

- [1] J. Clerk Maxwell, *A Treatise on Electricity and Magnetism*, 3rd ed., vol. 2. Oxford:Clarendon Press, 1892, pp.68-73.

Journals

- [2] Y. Yorozu, M. Hirano, K. Oka, and Y. Tagawa, “Electron spectroscopy studies on magneto-optical media and plastic substrate interface”, *IEEE Transl. J. Magn. Japan*, vol. 2, pp. 740-741, August 1987.

Conferences

- [3] Çolak I., Kabalci E., Bayindir R., and Sagiroglu S, “The design and analysis of a 5-level cascaded voltage source inverter with low THD”, *2nd PowerEng Conference*, Lisbon, pp. 575-580, 18-20 March 2009.

Reports

- [4] IEEE Standard 519-1992, Recommended practices and requirements for harmonic control in electrical power systems, *The Institute of Electrical and Electronics Engineers*, 1993.

Text Layout for Accepted Papers:

A4 page margins should be margins: top = 24 mm, bottom = 24 mm, side = 15 mm. Main text should be given in two column. The column width is 87mm (3.425 in). The space between the two columns is 6 mm (0.236 in). Paragraph indentation is 3.5 mm (0.137 in). Follow the type sizes specified in Table. Position figures and tables at the tops and bottoms of columns. Avoid placing them in the middle of columns. Large figures and tables may span across both columns. Figure captions should be centred below the figures; table captions should be centred above. Avoid placing figures and tables before their first mention in the text. Use the abbreviation “Fig. 1,” even at the beginning of a sentence.

Type size (pts.)	Appearance		
	Regular	Bold	<i>Italic</i>
10	Authors’ affiliations, Section titles, references, tables, table names, first letters in table captions, figure captions, footnotes, text subscripts, and superscripts	Abstract	
12	Main text, equations, Authors’ names, ^a		<i>Subheading (1.1.)</i>
24	Paper title		

Submission checklist:

It is hoped that this list will be useful during the final checking of an article prior to sending it to the journal's Editor for review. Please consult this Guide for Authors for further details of any item. Ensure that the following items are present:

- ❖ One Author designated as corresponding Author:
 - E-mail address
 - Full postal address
 - Telephone and fax numbers
- ❖ All necessary files have been uploaded
- Keywords: a minimum of 4
- All figure captions (supplied in a separate document)
- All tables (including title, description, footnotes, supplied in a separate document)
- ❖ Further considerations
 - Manuscript has been "spellchecked" and "grammar-checked"
 - References are in the correct format for this journal
 - All references mentioned in the Reference list are cited in the text, and vice versa

- Permission has been obtained for use of copyrighted material from other sources (including the Web)
- Color figures are clearly marked as being intended for color reproduction on the Web (free of charge) and in print or to be reproduced in color on the Web (free of charge) and in black-and-white in print.

Article Template Containing Author Guidelines for Peer-Review

First Author*, Second Author**‡, Third Author***

*Department of First Author, Faculty of First Author, Affiliation of First Author, Postal address

**Department of Second Author, Faculty of First Author, Affiliation of First Author, Postal address

***Department of Third Author, Faculty of First Author, Affiliation of First Author, Postal address

(First Author Mail Address, Second Author Mail Address, Third Author Mail Address)

‡Corresponding Author; Second Author, Postal address, Tel: +90 312 123 4567, Fax: +90 312 123 4567, corresponding@affl.edu

Received: xx.xx.xxxx Accepted:xx.xx.xxxx

Abstract- Enter an abstract of up to 250 words for all articles. This is a concise summary of the whole paper, not just the conclusions, and is understandable without reference to the rest of the paper. It should contain no citation to other published work. Include up to six keywords that describe your paper for indexing purposes. Define abbreviations and acronyms the first time they are used in the text, even if they have been defined in the abstract. Abbreviations such as IEEE, SI, MKS, CGS, sc, dc, and rms do not have to be defined. Do not use abbreviations in the title unless they are unavoidable.

Keywords- Keyword1; keyword2; keyword3; keyword4; keyword5.

2. Introduction

Authors should any word processing software that is capable to make corrections on misspelled words and grammar structure according to American or Native English. Authors may get help by from word

processor by making appeared the paragraph marks and other hidden formatting symbols. This sample article is prepared to assist authors preparing their articles to IJET.

Indent level of paragraphs should be 0.63 cm (0.24 in) in the text of article. Use single column layout, double-spacing and wide (3 cm) margins on white paper at the peer review stage. Ensure that each new paragraph is clearly indicated. Present tables and figure legends in the text where they are related and cited. Number all pages consecutively; use 12 pt font size and standard fonts; Times New Roman, Helvetica, or Courier is preferred. Indicate references by number(s) in square brackets in line with the text. The actual authors can be referred to, but the reference number(s) must always be given. Example: "..... as demonstrated [3, 6]. Barnaby and Jones [8] obtained a different result"

IJRER accepts submissions in three styles that are defined as Research Papers, Technical Notes and Letter, and Review paper. The requirements of paper are as listed below:

- Research Papers should not exceed 12 printed pages in two-column publishing format, including figures and tables.
- Technical Notes and Letters should not exceed 2,000 words.
- Reviews should not exceed 20 printed pages in two-column publishing format, including figures and tables.

Authors are requested write equations using either any mathematical equation object inserted to word processor or using independent equation software. Symbols in your equation should be defined before the equation appears or immediately following. Use "Eq. (1)" or "equation (1)," while citing. Number equations consecutively with equation numbers in parentheses flush with the right margin, as in Eq. (1). To make equations more compact, you may use the solidus (/), the exp function, or appropriate exponents. Italicize Roman symbols for quantities and variables, but not Greek symbols. Use an dash (–) rather than a hyphen for a minus sign. Use parentheses to avoid ambiguities in denominators. Punctuate equations with commas or periods when they are part of a sentence, as in

$$C = a + b \tag{1}$$

Section titles should be written in bold style while sub section titles are italic.

3. Figures and Tables

3.1. *Figure Properties*

All illustrations must be supplied at the correct resolution:

- Black and white and colour photos - 300 dpi
- Graphs, drawings, etc - 800 dpi preferred; 600 dpi minimum
- Combinations of photos and drawings (black and white and colour) - 500 dpi

In addition to using figures in the text, Authors are requested to upload each figure as a separate file in either .tiff or .eps format during submission, with the figure number as Fig.1., Fig.2a and so on. Figures are cited as “Fig.1” in sentences or as “Figure 1” at the beginning of sentence and paragraphs. Explanations related to figures should be given before figure. Figures and tables should be located at the top or bottom side of paper as done in accepted article format.



Figure 1. Engineering technologies.

Table captions should be written in the same format as figure captions; for example, “Table 1. Appearance styles.”. Tables should be referenced in the text unabbreviated as “Table 1.”

Table 1. Appearance properties of accepted manuscripts

Type size (pts.)	Appearance		
	Regular	Bold	<i>Italic</i>
10	Authors’ affiliations, Abstract, keywords, references, tables, table names, figure captions, footnotes, text subscripts, and superscripts	Abstract	
12	Main text, equations, Authors’ names, Section titles		<i>Subheading (1.1.)</i>
24	Paper title		

4. Submission Process

The *International Journal of Engineering Technologies* operates an online submission and peer review system that allows authors to submit articles online and track their progress via a web interface. Articles that are prepared referring to this template should be controlled according to submission checklist given in “Guide f Authors”. Editor handles submitted articles to IJET primarily in order to control in terms of compatibility to aims and scope of Journal.

Articles passed this control are checked for grammatical and template structures. If article passes this control too, then reviewers are assigned to article and Editor gives a reference number to paper. Authors registered to online submission system can track all these phases.

Editor also informs authors about processes of submitted article by e-mail. Each author may also apply to Editor via online submission system to review papers related to their study areas. Peer review is a critical element of publication, and one of the major cornerstones of the scientific process. Peer Review serves two key functions:

- Acts as a filter: Ensures research is properly verified before being published
- Improves the quality of the research

5. Conclusion

The conclusion section should emphasize the main contribution of the article to literature. Authors may also explain why the work is important, what are the novelties or possible applications and extensions. Do not replicate the abstract or sentences given in main text as the conclusion.

Acknowledgements

Authors may acknowledge to any person, institution or department that supported to any part of study.

References

- [1] J. Clerk Maxwell, *A Treatise on Electricity and Magnetism*, 3rd ed., vol. 2. Oxford:Clarendon Press, 1892, pp.68-73. (Book)
- [2] H. Poor, *An Introduction to Signal Detection and Estimation*, New York: Springer-Verlag, 1985, ch. 4. (Book Chapter)
- [3] Y. Yorozu, M. Hirano, K. Oka, and Y. Tagawa, "Electron spectroscopy studies on magneto-optical media and plastic substrate interface", *IEEE Transl. J. Magn. Japan*, vol. 2, pp. 740-741, August 1987. (Article)
- [4] E. Kabalci, E. Irmak, I. Çolak, "Design of an AC-DC-AC converter for wind turbines", *International Journal of Energy Research*, Wiley Interscience, DOI: 10.1002/er.1770, Vol. 36, No. 2, pp. 169-175. (Article)
- [5] I. Çolak, E. Kabalci, R. Bayindir R., and S. Sagiroglu, "The design and analysis of a 5-level cascaded voltage source inverter with low THD", *2nd PowerEng Conference*, Lisbon, pp. 575-580, 18-20 March 2009. (Conference Paper)
- [6] IEEE Standard 519-1992, Recommended practices and requirements for harmonic control in electrical power systems, *The Institute of Electrical and Electronics Engineers*, 1993. (Standards and Reports)

Article Template Containing Author Guidelines for Accepted Papers

First Author*, Second Author**[‡], Third Author***

*Department of First Author, Faculty of First Author, Affiliation of First Author, Postal address

**Department of Second Author, Faculty of First Author, Affiliation of First Author, Postal address

***Department of Third Author, Faculty of First Author, Affiliation of First Author, Postal address

(First Author Mail Address, Second Author Mail Address, Third Author Mail Address)

[‡]Corresponding Author; Second Author, Postal address, Tel: +90 312 123 4567,

Fax: +90 312 123 4567,corresponding@affl.edu

Received: xx.xx.xxxx Accepted:xx.xx.xxxx

Abstract- Enter an abstract of up to 250 words for all articles. This is a concise summary of the whole paper, not just the conclusions, and is understandable without reference to the rest of the paper. It should contain no citation to other published work. Include up to six keywords that describe your paper for indexing purposes. Define abbreviations and acronyms the first time they are used in the text, even if they have been defined in the abstract. Abbreviations such as IEEE, SI, MKS, CGS, sc, dc, and rms do not have to be defined. Do not use abbreviations in the title unless they are unavoidable.

Keywords Keyword1, keyword2, keyword3, keyword4, keyword5.

1. Introduction

Authors should use any word processing software that is capable to make corrections on misspelled words and grammar structure according to American or Native English. Authors may get help by using word processor by making sure the paragraph marks and other hidden formatting symbols. This sample article is prepared to assist authors preparing their articles to IJRER.

Indent level of paragraphs should be 0.63 cm (0.24 in) in the text of article. Use single column layout, double-spacing and wide (3 cm) margins on white paper at the peer review stage. Ensure that each new paragraph is clearly indicated. Present tables and figure legends in the text where they are related and cited. Number all pages consecutively; use 12 pt font size and standard fonts; Times New Roman, Helvetica, or Courier is preferred. Indicate references by number(s) in square brackets in line with the text. The actual authors can be referred to, but the reference number(s) must always be given. Example: "..... as demonstrated [3,6]. Barnaby and Jones [8] obtained a different result"

IJRER accepts submissions in three styles that are defined as Research Papers, Technical Notes and Letter, and Review paper. The requirements of paper are as listed below:

➤ Research Papers should not exceed 12 printed pages in two-column publishing format, including figures and tables.

➤ Technical Notes and Letters should not exceed 2,000 words.

➤ Reviews should not exceed 20 printed pages in two-column publishing format, including figures and tables.

Authors are requested write equations using either any mathematical equation object inserted to word processor or using independent equation software. Symbols in your equation should be defined before the equation appears or immediately following. Use "Eq. (1)" or "equation (1)," while citing. Number equations consecutively with equation numbers in parentheses flush with the right margin, as in Eq. (1). To make equations more compact, you may use the solidus (/), the exp function, or appropriate exponents. Italicize Roman symbols for quantities and variables, but not Greek symbols. Use an dash (-) rather than a hyphen for a minus sign. Use parentheses to avoid ambiguities in denominators. Punctuate equations with commas or periods when they are part of a sentence, as in

$$C = a + b \quad (1)$$

Section titles should be written in bold style while sub section titles are italic.

6. Figures and Tables

6.1. Figure Properties

All illustrations must be supplied at the correct resolution:

- Black and white and colour photos - 300 dpi
- Graphs, drawings, etc - 800 dpi preferred; 600 dpi minimum
- Combinations of photos and drawings (black and white and colour) - 500 dpi

In addition to using figures in the text, Authors are requested to upload each figure as a separate file in either .tiff or .eps format during submission, with the figure number as Fig.1., Fig.2a and so on. Figures are cited as “Fig.1” in sentences or as “Figure 1” at the beginning of sentence and paragraphs. Explanations related to figures should be given before figure.



Fig. 1. Engineering technologies.

Figures and tables should be located at the top or bottom side of paper as done in accepted article format. Table captions should be written in the same format as figure captions; for example, “Table 1. Appearance styles.”. Tables should be referenced in the text unabbreviated as “Table 1.”

Table 1. Appearance properties of accepted manuscripts

Type size (pts.)	Appearance		
	Regular	Bold	<i>Italic</i>
10	Main text, section titles, authors’ affiliations, abstract, keywords, references, tables, table names, figure captions, equations, footnotes, text subscripts, and superscripts	Abstract-	<i>Subheading (1.1.)</i>
12	Authors’ names,		
24	Paper title		

6.2. Text Layout for Accepted Papers

A4 page margins should be margins: top = 24 mm, bottom = 24 mm, side = 15 mm. The column width is 87mm (3.425 in). The space between the two columns is 6 mm (0.236 in). Paragraph indentation is 3.5 mm (0.137 in). Follow the type sizes specified in Table. Position figures and tables at the tops and bottoms of columns. Avoid placing them in the middle of columns. Large figures and tables may span across both columns. Figure captions should be centred below the figures; table captions should be centred above. Avoid placing figures and tables before their first mention in the text. Use the abbreviation “Fig. 1,” even at the beginning of a sentence.

7. Submission Process

The International Journal of Renewable Energy Research operates an online submission and peer review system that allows authors to submit articles online and track their

progress via a web interface. Articles that are prepared referring to this template should be controlled according to submission checklist given in “Guide f Authors”. Editor handles submitted articles to IJRER primarily in order to control in terms of compatibility to aims and scope of Journal. Articles passed this control are checked for grammatical and template structures. If article passes this control too, then reviewers are assigned to article and Editor gives a reference number to paper. Authors registered to online submission system can track all these phases. Editor also informs authors about processes of submitted article by e-mail. Each author may also apply to Editor via online submission system to review papers related to their study areas. Peer review is a critical element of publication, and one of the major cornerstones of the scientific process. Peer Review serves two key functions:

- Acts as a filter: Ensures research is properly verified before being published
- Improves the quality of the research

8. Conclusion

The conclusion section should emphasize the main contribution of the article to literature. Authors may also explain why the work is important, what are the novelties or possible applications and extensions. Do not replicate the abstract or sentences given in main text as the conclusion.

Acknowledgements

Authors may acknowledge to any person, institution or department that supported to any part of study.

References

- [7] J. Clerk Maxwell, A Treatise on Electricity and Magnetism, 3rd ed., vol. 2. Oxford:Clarendon Press, 1892, pp.68-73. (Book)
- [8] H. Poor, An Introduction to Signal Detection and Estimation, New York: Springer-Verlag, 1985, ch. 4. (Book Chapter)
- [9] Y. Yorozu, M. Hirano, K. Oka, and Y. Tagawa, "Electron spectroscopy studies on magneto-optical media and plastic substrate interface", IEEE Transl. J. Magn. Japan, vol. 2, pp. 740-741, August 1987. (Article)
- [10] E. Kabalcı, E. Irmak, I. Çolak, "Design of an AC-DC-AC converter for wind turbines", International Journal of Energy Research, Wiley Interscience, DOI: 10.1002/er.1770, Vol. 36, No. 2, pp. 169-175. (Article)
- [11] I. Çolak, E. Kabalcı, R. Bayindir R., and S. Sagirolu, "The design and analysis of a 5-level cascaded voltage source inverter with low THD", 2nd PowerEng Conference, Lisbon, pp. 575-580, 18-20 March 2009. (Conference Paper)
- [12] IEEE Standard 519-1992, Recommended practices and requirements for harmonic control in electrical power systems, The Institute of Electrical and Electronics Engineers, 1993. (Standards and Reports)

**INTERNATIONAL JOURNAL OF ENGINEERING TECHNOLOGIES (IJET)
COPYRIGHT AND CONSENT FORM**

This form is used for article accepted to be published by the IJET. Please read the form carefully and keep a copy for your files.

TITLE OF ARTICLE (hereinafter, "The Article"):

.....
.....
.....

LIST OF AUTHORS:

.....
.....
.....

CORRESPONDING AUTHOR'S ("The Author") NAME, ADDRESS, INSTITUTE AND EMAIL:

.....
.....
.....

COPYRIGHT TRANSFER

The undersigned hereby transfers the copyright of the submitted article to International Journal of Engineering Technologies (the "IJET"). The Author declares that the contribution and work is original, and he/she is authorized by all authors and/or grant-funding agency to sign the copyright form. Author hereby assigns all including but not limited to the rights to publish, distribute, reprints, translates, electronic and published derivatives in various arrangements or any other versions in full or abridged forms to IJET. IJET holds the copyright of Article in its own name.

Author(s) retain all rights to use author copy in his/her educational activities, own websites, institutional and/or funder's web sites by providing full citation to final version published in IJET. The full citation is provided including Authors list, title of the article, volume and issue number, and page number or using a link to the article in IJET web site. Author(s) have the right to transmit, print and share the first submitted copies with colleagues. Author(s) can use the final published article for his/her own professional positions, career or qualifications by citing to the IJET publication.

Once the copyright form is signed, any changes about the author names or order of the authors listed above are not accepted by IJET.

Authorized/Corresponding Author

Date/ Signature